学位論文

Theoretical study of superconductivity in ladder systems with even and odd number of legs

偶奇本梯子系における超伝導の理論的研究

平成８年１２月博士（理学）申請

東京大学大学院理学系研究科
物理学専攻

木村　敬

学位論文

Theoretical study of superconductivity in ladder systems with even and odd number of legs

偶奇本梯子系における超伝導の理論的研究

平成８年１２月博士（理学）申請

東京大学大学院理学系研究科
物理学専攻

木村　敬

Acknowledgments

The author would like to express his sincere gratitude to Professor Hideo Aoki for his guidance to many-body problems in solid state physics, helpful discussions and suggestions, and the critical reading of the manuscript. His special thanks are also due to Dr. K. Kuroki for valuable discussions and technical supports which are indispensable to the present thesis.

The author is pleased to acknowledge helpful communications with Professors M. Fabrizio, A.M. Finkelstein, G. Fasol, M. Ogata, H.J. Schulz, E. Arrigoni, Y. Takada, H. Fukuyama, M. Imada, N. Môri, and A. Fujimori. He also acknowledges all the professors in Department of Physics in Sophia University and the theorists in Department of Physics in Gakushuin University for guiding him to theoretical physics when he was an undergraduate student.

The author acknowledges Professor M. Tsukada for helpful suggestions. He also thanks all the members and the seniorities of the research group under Professors Tsukada and Aoki for fruitful discussions, helpful suggestions, and encouragements.

Numerical calculations were done on FACOM VPP 500/40 at the Supercomputer Center, Institute for Solid State Physics, the University of Tokyo and on HITAC S3800/280 at the Computer Center of the University of Tokyo. For the latter facility the author thanks Prof. Y. Kanada for a support in 'Project for Vectorized Super Computing'. This work was also supported in part by Grand-in-Aid for Scientific Research from the Ministry of Education, Science, Sports, and Culture of Japan. The author acknowledges the Japan Society for the Promotion of Science for a fellowship.

Last but not least, the author acknowledges his parents for their financial supports and encouragements.

Contents

Chapter 1

Introduction

Since its discovery by Kamerlingh Onnes[1], superconductivity has been examined as one of the most fascinating phenomena in solid state physics. The most famous and successful theory of superconductivity was given by Bardeen, Cooper and Schrieffer [2] in 1957, the theory now well known as the BCS theory. The BCS theory is based on the phonon mediated attraction between electrons and explains most properties of superconductors not only qualitatively but also quantitatively.

On the other hand, there is a history of the quest for mechanism due to repulsive interactions between electrons rather than the phonon mediated attractions. Indeed, there are some widely noticed mechanisms with effective attractions mediated by bosonic collective excitations, plasmons (charge fluctuations)[3], anti-ferromagnetic spin fluctuations[4, 5], and so on. The study of such electronic mechanisms received an impetus from the discovery of the high-T_C superconductor[6], which may require a mechanism other than BCS.

Although the high-T_C superconductor has among of such as the magnitude of the transition temperature from conventional superconductors, one of the most important differences is the "anomalous" normal-state properties in the lightly-doped regime [7]. The unusual properties, which are not expected from conventional Fermi liquids, include resistivity[8, 9, 10], optical conductivity[11, 12, 13], Hall coefficient[9, 10, 14], and NMR [15, 16, 17, 18]. It is widely believed that understanding the unusual normal state properties of the high-T_c cuprates will elucidate the superconducting mechanism. Recently, the presence of a "spin-gap" in the normal state has been regarded as an important key to understand the normal state properties, such as the magnetic properties (Fig.1.1), and further the superconducting mechanism.

To understand the cuprates, both the Hubbard and the $t-J$ models have been extensively studied as effective Hamiltonians for the low-energy excitations on the two-dimensional (2D) CuO_2 plane, on which the carriers reside[19].

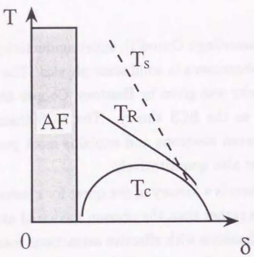

Figure 1.1: Magnetic phase diagram on the plane of doping δ and temperature in cuprates; T_s, the onset temperature of the suppression of the magnetic susceptibility, T_R, the temperature where the NMR rate $1/(T_1T)$ takes maximum value, T_C, the superconducting transition temperature.

The single-band Hubbard model, which was proposed as an effective model for the cuprate by Anderson[20], is described by the Hamiltonian,

$$H = -t \sum_{<i,j>\sigma} c^{\dagger}_{i,\sigma} c_{j,\sigma} + U \sum_{i} n_{i\uparrow} n_{i\downarrow}. \quad (1.1)$$

Here $c^{\dagger}_{i,\sigma}(c_{i,\sigma})$ is the creation (annihilation) operator of an electron of spin σ at site i, t is the transfer energy, U is the on-site interaction, $n_{i\sigma} = c^{\dagger}_{i\sigma} c_{i\sigma}$ and $< i, j >$ denotes nearest neighbor sites. Actually, the relation between the Hubbard model and the cuprates is not clear, since the Hubbard model is an approximate model that roughly neglects the oxygen sites in the cuprates. Initially, however, the Hubbard model has been widely discussed since 1960's especially as a relevant model for the magnetism in the transition metals[21], and its ground state has also been widely discussed. Thus, the Hubbard model is one of the prototypes for strongly-correlated-electron systems. Superconductivity in the 2D Hubbard model has been extensively discussed both analytically[22, 23, 24, 25, 26] and numerically[27, 28, 29, 30, 31, 32, 33, 34]. Some analytical calculations support the dominance of pairing correlations in the doped systems. However, the quantum Monte Carlo (QMC) method, which enables us to obtain correlation functions for relatively large systems, shows that there is no enhancement of the pairing correlation at any fillings[28, 29]. Thus the dominance of a pairing correlation in the 2D Hubbard model seems unlikely in numerical calculations, as far as pairing correlation of the bare electrons are considered.

On the other hand, the $t - J$ model is given by the Hamiltonian,

$$H = -t \sum_{<i,j>\sigma} \tilde{c}^{\dagger}_{i,\sigma} \tilde{c}_{j,\sigma} + J \sum_{<i,j>} \mathbf{S}_i \cdot \mathbf{S}_j. \quad (1.2)$$

Here J is the super-exchange interaction via the oxygen atom and $\tilde{c}_{i,\sigma} = c_{i,\sigma}(1 - n_{i,-\sigma})$, etc. The limit of small J/t corresponds to the large-U limit of the Hubbard model. Mean-field theory based on the slave-boson approach [35, 36, 37] shows the occurrence of superconductivity in the 2D $t - J$ model. In the slave-boson approach, the onset temperature of the singlet pairing of the spinon, which is the spin-fermion field of the decomposed electron field, corresponds to the temperature at which the spin gap is created. The dominance of the pairing correlation in the $t - J$ model is also confirmed for relatively large J/t by numerical calculations [38, 39, 40, 41, 42, 43, 44]. In relation to the formation of the spin gap, extended $t - J$ models such as the dimerized $t - J$ ($t - J$ model with dimerized spin-spin coupling[45, 46]) or $t - J - V$ ($t - J$ model with nearest neighbor repulsion[47, 48, 49]) models, have also been of great interest.

In an effort to understand strongly-correlated systems one dimensional (1D) systems have also been studied extensively, although their connection to 2D systems has to be worked out. It is now widely understood that the 1D systems are in general described not as the Fermi liquid but as the *Tomonaga-Luttinger liquid* (the TL liquid) in low energy regime[50, 51, 52]. This was shown in the weak-coupling regime by the bosonization[51, 52] combined with the renormalization group methods[50] in the 1970's. In 1982, Haldane conjectured that the 1D electron systems are generally expressed as the TL liquids [53, 54, 55, 56]. This conjecture has been recently confirmed by the conformal field theory[57, 58] combined with Bethe Ansatz method for both the Hubbard[59] and the super-symmetric $t-J$ models[60, 61, 62].

The TL liquid has important properties different from those for the Fermi liquid. Above all, the spin and the charge degrees of freedoms are completely decoupled in the TL liquid. This is called *the spin-charge separation*. Another important difference is that the TL liquid has no quasi-particle excitations and all of the excitations are collective ones. Nature of the ground state is characterized by the long-range part of the correlation functions, which can be exactly calculated in the TL liquid. Generally speaking, strong quantum fluctuations prevent the occurrence of true long-range order even at $T = 0$ in 1D, so that correlation functions vanish at long distances, except for the special case such as ferromagnetic long-range order in the ferromagnetic Heisenberg model, in which the order parameter commutes with the Hamiltonian. However, we may consider that the order which has the most slowly-decaying correlation function will be realized in real systems which must have some three-dimensional (3D) properties.

The ground state of the TL liquid which corresponds to the Hubbard model with repulsive interactions or the $t-J$ model with a small exchange coupling cannot exhibit superconductivity[63], since the dominant correlation is that of the spin-density wave (SDW). Physically, the reason why there is no dominating pairing correlation is that there is no gapful spin mode in 1D, since the only spin mode becomes gapless.

Over the past several years, the systems with quasi-1D ladder structures have been received much attention. Cuprate compounds containing such structures have been fabricated recently[64]. The undoped system is a Mott insulator and can be considered as an anti-ferromagnetic (AF) Heisenberg spin-ladder system. In 1986, Schulz[65] first conjectured that an AF spin-ladder system with n-legs is very similar to a 1D AF $S = N/2$ spin-chain system (Haldane system)[65, 66, 67, 68]. Namely, even-numbered-leg ladders which correspond to a 1D spin chain of integer spins should be a spin liquid with the spin excitations being gapful, while odd-numbered leg ladders which correspond to half-odd-integer spins should be antiferromagnetic with the spin excitations being gapless. Both theoretical[70, 71, 72, 73, 74, 75, 76, 77, 78, 79, 80] and experimental[81, 82, 83, 84, 85, 86, 87, 88] studies on the undoped-ladder systems have supported this conjecture, especially after the similar proposal by Rice et al.[89] as mentioned below.

In real systems, for example, $Sr_{n-1}Cu_{n+1}O_{2n}$ has an n-leg-ladder structure on CuO_2 plane. Recent experiments on $SrCu_2O_3$ and $Sr_2Cu_3O_5$ have confirmed the conjecture[83, 84, 85, 86, 87]. Namely, the two-leg-ladder system $SrCu_2O_3$ shows a spin-liquid behavior characteristic of a finite spin-correlation length, while the three-leg system $Sr_2Cu_3O_5$ shows an AF behavior (Figures 1.2 and 1.3). Furthermore the spin-ladder systems may

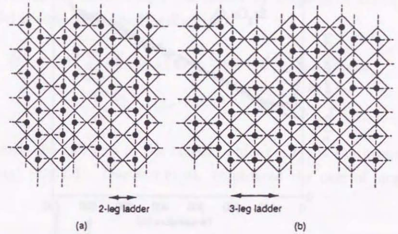

Figure 1.2: Schematic ladder structures; (a) a two-leg ladder, (b) a three-leg ladder.

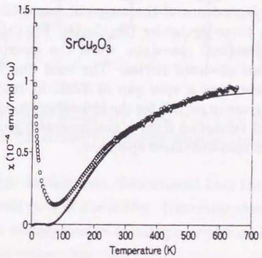

(a)

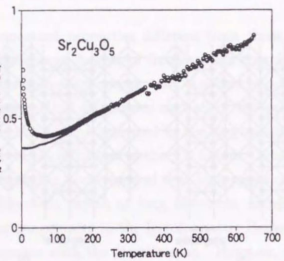

(b)

Figure 1.3: Temperature dependence of the magnetic susceptibility of a two-leg ladder ($SrCu_2O_3$, Fig.(a)) and a three-leg ladder ($Sr_2Cu_3O_5$, Fig.(b)) given in ref.[84]. The open circles are the experimental raw data, while the data after subtraction of the Curie component are shown as closed circles. The solid line in Fig.(a) represents the calculated susceptibility assuming a spin gap of 420K in ref.[84], using the equation $\chi(T) \propto T^{-1/2}\exp(-\Delta/T)$ given in ref.[78] for the Heisenberg ladder. The data of $SrCu_2O_3$ is characteristic of thermal excitation from a non-magnetic ground state, while that of $Sr_2Cu_3O_5$ reflects a gapless spin-excitation spectrum.

contain some clues for understanding the high-T_C cuprates, especially for the role of the spin gap. In connection with the spin gap, the impurity effect which removes the spin gap in the two-leg ladder is also of interest[90, 91].

For superconductivity we have to consider carrier-doped systems. Rice et al. gave a conjecture similar to Schulz's for undoped systems and further have conjectured for doped systems that an even-numbered ladder should exhibit dominance of the inter-ladder singlet-pairing correlation as expected from the persistent spin gap away from half-filling[89]. The conjecture is partly based on the numerical exact-diagonalization study for finite systems for the two-leg $t-J$ ladder by Dagotto et al.[70]. The two-leg $t-J$ ladder model is defined by the Hamiltonian,

$$\begin{aligned} H &= -t\sum_{i,\alpha,\sigma}(\tilde{c}^{\dagger}_{i,\alpha,\sigma}\tilde{c}_{i+1,\alpha,\sigma}+\text{h.c.}) + J\sum_{i,\alpha}\mathbf{S}_{i,\alpha}\cdot\mathbf{S}_{i+1,\alpha} \\ &\quad -t_{\perp}\sum_{i,\sigma}(\tilde{c}^{\dagger}_{i,1,\sigma}\tilde{c}_{i,2,\sigma}+\text{h.c.}) + J_{\perp}\sum_{i}\mathbf{S}_{i,1}\cdot\mathbf{S}_{i,2}. \end{aligned} \quad (1.3)$$

Here $\alpha(=1,2)$ labels the two legs of the ladder, while $t_{\perp}(J_{\perp})$ is the interchain hopping (exchange coupling) (Fig.1.4). Dagotto et al. considered the case of large $J_{\perp}$ limit at

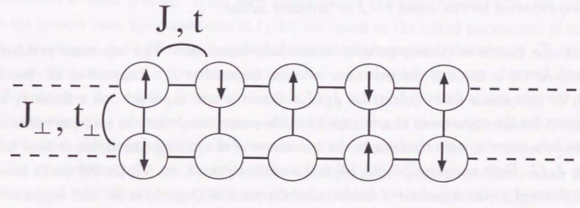

Figure 1.4: Two-leg $t-J$ ladder model; $t(t_{\perp})$ and $J(J_{\perp})$ are the intrachain (interchain) hopping and the intrachain (interchain) exchange coupling, respectively.

half-filling in the beginning. In this case, they showed that the ground state consists of a set of spin singlets on each rung of the ladder. Naturally, there is a gap of order $J_{\perp}$ in the spin excitations which corresponds to creating a triplet on one of the rungs and the system will be a spin liquid rather than AF.

When the system is hole doped, it is also energetically favorable to break as few singlet pairs as possible. The resultant liquid of singlets is expected to retain a spin gap, where the energy gained by putting the holes in pairs may be regarded as a hole-pair-binding energy so that the dominance of the pairing correlation is expected. The pairing operator of superconductivity is an off-site one and represented as

$\Delta_i = \tilde{c}_{i1\uparrow}\tilde{c}_{i2\downarrow} - \tilde{c}_{i1\downarrow}\tilde{c}_{i2\uparrow}$.

Δ is represented in momentum space as

$\Delta = \sum_{k\sigma} \sigma(\tilde{c}_{0k\sigma}\tilde{c}_{0-k-\sigma} - \tilde{c}_{\pi k\sigma}\tilde{c}_{\pi-k-\sigma})$.

Namely, the pairing, in addition to being off-site, consists of both the bonding (0) and the anti-bonding (π) bands that interfere with opposite signs, so that the pairing may be called *d-wave-like pairing* (Fig.1.5). This reminds us that the d-wave pairing is expected

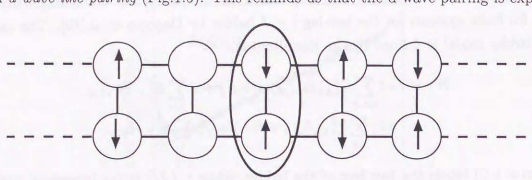

Figure 1.5: Schematic picture for the interchain *d-wave-like* pairing (in the ellipse in the figure) expected for the doped $t-J$ or Hubbard ladder.

in high-T_C superconductors especially for the hole-doped case. The important problem is both the spin gap and the pairing correlation for smaller $J_\perp$. Dagotto et al. found that the spin gap is finite at least for $J_\perp/J > 0.4$ (it is now expected that a finite $J_\perp$ is sufficient for the appearance of spin gaps[72]). They also found that the spin gap remains in the hole-doped system resulting in the dominance of the pairing correlation at least for large $J_\perp/J$. Both analytical[92, 93, 94] and numerical[76, 95, 96, 97, 98, 99] works have been devoted to the doped $t-J$ ladder after the work of Dagotto et al. and supported the dominant pairing correlation in a certain region. Generally speaking, the dominant paring correlation appears at lower values of exchange couplings than in the case of a single chain.

From an experimental point of view, it had been difficult to observe superconductivity in two-leg ladder systems. In fact, Hiroi and Takano[100] reported that a ladder material $LaCuO_{2.5}$ showed clear insulator-metal transition upon hole carrier doping by substitution of Sr^{2+} for La^{3+} but no sign of superconductivity was observed. Localization of the carriers due to strong random potential may disturb the superconducting transition as discussed in the above report[100].

However, more recently, Uehara et al.[101] have observed superconductivity in

$Sr_{0.4}Ca_{13.6}Cu_{24}O_{41.84}$ under high pressure of 3 GPa and 4.5 GPa (Fig.1.6 and Fig.1.7). It is an important advantage of the high pressure technique that it can change the parameters of the system without increase of the randomness, although how the high pressure changes the parameters is not so clear.

Theoretically, the Hubbard model on ladders have also been of interest, recently. The Hubbard ladder model is defined by the Hamiltonian,

$$\begin{aligned} H &= -t\sum_{i,\alpha,\sigma}(c^\dagger_{i,\alpha,\sigma}c_{i+1,\alpha,\sigma} + \text{h.c.}) \\ &\quad -t_\perp\sum_{i,\sigma}(c^\dagger_{i,1,\sigma}c_{i,2,\sigma} + \text{h.c.}) + U\sum_{i,\alpha} n_{i,\alpha,\uparrow}n_{i,\alpha,\downarrow}. \end{aligned} \tag{1.4}$$

Here, $t(t_\perp)$ is the intrachain(interchain) hopping and U is the on-site repulsion, respectively. (Fig.1.8). Since the Bethe Ansatz is not applicable to the Hubbard ladder with two or larger numbers of legs, its treatment requires some kinds of approximations. The most reliable analytical method is the perturbational renormalization-group method [50, 103, 104], which takes the continuum limit of the system, linearizes the band structure around the Fermi points, and treats the interaction with a perturbative renormalization group. The method was established for treating the correlated 1D electron gas in the 1970's and is called '*g-ology*'. It has been used for some two-band systems [105, 106, 107]. In the present case, the parameters $(t, t_\perp, U)$ are taken as the initial parameters of coupling constants. As a point to notice in the weak-coupling theory, we should note that the non-interacting system and the system in the weak-coupling limit $U \to +0$ are quite different, since for a finite U the relevant coupling constants, which correspond to the relevant scattering processes, are renormalized to infinity and the initial value of U only affects some couplings which are invariant in the renormalization flow, if the fixed point of the renormalization is not changed. (The infinitely-large coupling constants mean the existence of infinitely-large excitation gap and the absence of the correlation lengths. This is not inconsistent with the lattice systems because there are infinite number of sites in the continuum limit, so that an infinitely large excitation gap in a continuum system corresponds to a finite excitation gap in lattice system.) As an example, we can remember the 1D attractive($U \leq 0$) Hubbard model, in which a finite $U(\leq 0)$ is sufficient for a finite spin gap to open, and the exponent of the singlet pairing correlation is discontinuously reduced to unity, while the exponent is twice as large in the non-interacting case.

However, there is a serious problem for the weak-coupling theory. First, whether the model in the continuous limit is equivalent to the lattice model is not obvious. More serious is the problem that the perturbational renormalization group is guaranteed only for an infinitesimally small interaction strengths in principle. Specifically, when there is a

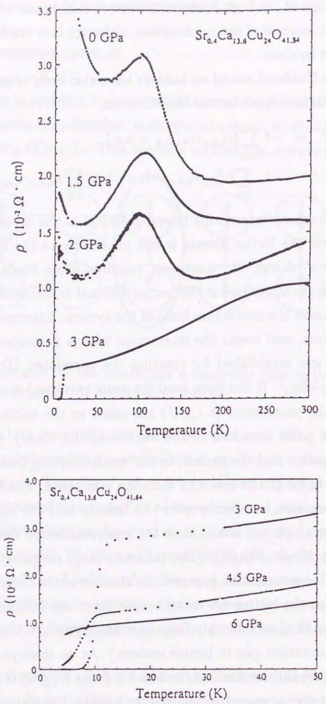

Figure 1.6: Temperature dependence of the electrical resistivities ρ of $Sr_{0.4}Ca_{13.6}Cu_{24}O_{41.84}$ under pressures of 0, 1.5, 2, 3, 4.5, 6 GPa given in ref.[101]. The electrical resistivities disappear under pressures of 3, 4.5 GPa at low temperatures.

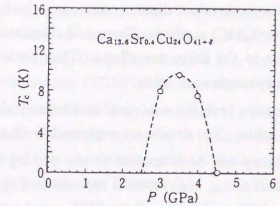

Figure 1.7: Schematic diagram given in ref.[102] for the relation between the superconducting transition temperature T_C and the pressure.

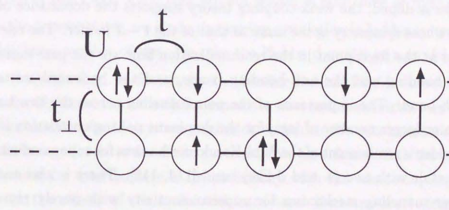

Figure 1.8: Two-leg Hubbard ladder model; $t(t_\perp)$ and U are the intrachain(interchain) hopping and the on-site interaction, respectively.

gap in the excitation, the renormalization flows into a strong-coupling regime, so that the perturbation theory might break down even for small U. A way to check the reliability of the weak-coupling theory is to treat finite-size systems with larger U with numerical calculations such as exact diagonalization, density-matrix renormalization group (DMRG), and quantum Monte Carlo (QMC) methods. Numerical calculations, on the other hand, have serious problems due to the finite size effects. Thus both the analytical and the numerical calculations compensate each other.

Now, we briefly summarize both the analytical and numerical results obtained so far for the two-leg Hubbard ladder. The details are explained in Chapter 2.

The weak-coupling theory has been applied to the two-leg Hubbard ladder model [108, 109, 110, 111]. At half-filling, the system is reduced to a spin-liquid insulator with both charge and spin gaps[108] leading to a finite SDW correlation length.

One might expect that the Hubbard ladder would not exhibit a sizeable spin gap at half-filling unlike the $t-J$ ladder, which is equivalent to the Heisenberg ladder at half-filling by definition, with a large J. However, the spin gap for the Hubbard model estimated in a DMRG study by Noack et al.[112, 113] is as large as $0.13t(\sim$ 400K for $t \sim 0.3$eV) for $U=8t$ (with $t=t_{\perp}$, which is of interest as a model relevant to cuprates). The magnitude of the spin gap is comparable with the spin gap ($\sim$ 400K) experimentally estimated from the magnitude of susceptibility for $SrCu_2O_3$. Noack et al. showed that the two-leg Hubbard ladder is also an spin liquid insulator for all U and $t_{\perp} < 2t$, while the system is a band insulator for $t_{\perp} > 2t$.

When the carrier is doped, the weak-coupling theory supports the dominance of the pairing correlation whose symmetry is the same as that of the $t-J$ ladder. The relevant scattering processes at the fixed point in the renormalization flow are the pair-tunneling process across the bonding and the anti-bonding bands, and the backward-scattering process within each band. The importance of the pair-tunneling across the two bands, which exists in two or larger number of legs, for the dominant pairing correlation in the two-leg Hubbard ladder is reminiscent of the Suhl-Kondo mechanism for superconductivity in the transition metals with two (s- and d-like) bands[114, 115]. There is also another example of the pair-tunneling mechanism for superconductivity with purely repulsive interactions. Muttalib and Emery[116] considered a two-band 1D electron gas with an interband pair-tunneling and found that the model is exactly solvable at special points and that pairing correlation can become dominant even if all the coupling constants are positive.

The properties of the weak-coupling Hubbard ladder are similar to those of the $t-J$

ladder for the regime where the pairing correlation is dominant, since in addition to the existence of the spin gap, the exponent for the pairing correlation should be reciprocal to that for the subdominant $4k_F$ CDW (*duality relation*[110, 111]) in both the weak-coupling theory and the two-leg $t-J$ ladder[96, 97, 99]. The reason may be that the form of the excitation gaps in the bosonization description in the $t-J$ ladder and that in the Hubbard ladder are the same[110]. Namely, the gapless mode is only one charge mode and no spin modes are gapless in both systems ('C1S0' phase in terms of the weak-coupling theory).

However, the dominance of the pairing correlation is a subtle problem in numerical calculations. Existing numerical results appear to be controversial [112, 125, 113, 117, 118] and some of them also seem to be inconsistent with the weak-coupling theory. The details will be presented in the introduction of Chapter 2.

Apart from the above mentioned inconsistencies, most of the existing theories support the dominance of the pairing correlation in the doped two-leg ladders. Then, an even more important unresolved problem for superconductivity in the doped ladder systems may be the 'even-odd' problem. One can naively expect an absence of dominating pairing correlation for systems with odd numbers of legs, in which the spin gap is absent in contrast to the case of even numbers of legs. The single chain, which is the simplest example of odd number of legs, does not indeed exhibit a dominant pairing correlation. However, no studies have looked into the pairing correlation functions for the three or larger odd number of legs, although White et al.[119] study the cases in which two holes are doped in the multi-leg $t-J$ ladder at half-filling: two holes doped are bound in even(two or four) legs, while they are not bound in odd(three or five) legs.

In the present thesis, we study the pairing correlation in ladder systems with even(two) or odd(three) number of legs. We take the Hubbard model as a model Hamiltonian.

In the beginning, we first study the two-leg Hubbard ladder model[120]. In order to study the Hubbard ladder with intermediate interaction strengths, we have performed a QMC calculation for the system paying attention to the non-interacting ($U=0$) single-particle energy levels in the finite systems. We have found that the pairing correlation is enhanced for intermediate U in consistency with the weak-coupling theory. Further we check the effects of the inter- and intra-band Umklapp-scattering processes, which are expected from the weak-coupling theory[108] at the special band fillings where the Umklapp processes may be relevant.

Secondly, we study an odd (three)-leg Hubbard ladder model (Fig.1.9) with the weak-coupling theory[121] using the enumeration of gapless modes by Arrigoni[122]. The system has one gapless spin mode and two gapful spin modes. Thus the gapful and the gapless

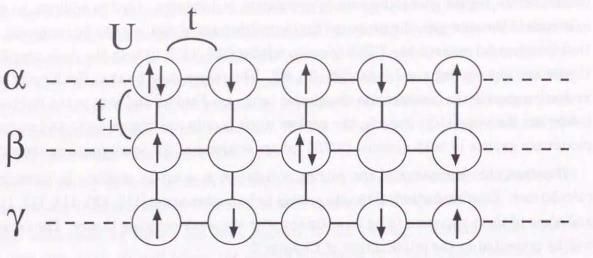

Figure 1.9: Three-leg Hubbard ladder model; $t(t_\perp)$ and U are the intrachain (interchain) hopping and the on-site interaction, respectively.

spin modes coexist. The existence of the gapful modes is a result of the relevant interband pair-tunneling process across the top and the bottom bands. As a result, we find the dominance of the pairing correlation across the central and the edge chains reflecting the gapful spin modes, which coexists with the subdominant but power-law decaying SDW correlation reflecting the gapless spin mode. Thus the Suhl-Kondo-like mechanism for superconductivity survives not only in even-leg systems but also in an odd(three)-leg system, while the SDW correlation also survives as expected. Schulz[123] also found similar results independently.

However the result is again confined within the weak-coupling theory. Thus, we finally study the three-leg Hubbard ladder model by a QMC calculation[124] as in the two-leg case. The technique to detect the enhanced pairing correlation in the two-leg case is also valid in the three-leg case. We found that the enhancement of the pairing correlation persists for the intermediate interaction strengths. We also study the effects of the Umklapp processes at special band fillings as in the two-leg case.

The organization of the present thesis is as follows. The QMC study for the two-leg Hubbard ladder is given in Chapter 2. In Chapter 3, we study the three-leg Hubbard ladder within the weak-coupling theory. In Chapter 4, the QMC study for the three-leg Hubbard ladder is given. Finally, the conclusions of the present thesis are given in Chapter 5. Both the QMC and the analytical calculations adopted in the present thesis are described in Appendices.

Chapter 2

Quantum Monte Carlo study of the pairing correlation in the two-leg Hubbard ladder

In this chapter, an extensive quantum Monte Carlo calculation is performed for the two-leg Hubbard ladder model to clarify whether the singlet pairing correlation decays slowly, which is predicted from the weak-coupling theory but controversial from numerical studies. We pay attention to the non-interacting single particle energy levels in finite system. Our result suggest that the discreteness of energy levels in finite systems affects the correlation enormously, where the enhanced pairing correlation is indeed detected if we make the energy levels of both the bonding and the anti-bonding bands aligned at the Fermi level to mimic the thermodynamic limit. We also study the effects of the Umklapp processes at special fillings as an effect of fillings.

2.1 Introduction

As stated in Chapter 1, strongly correlated electrons on ladders have received much attention both theoretically and experimentally [64]. Especially for the two-leg ladder, the theoretical studies suggest the formation of a spin gap and the possible occurrence of superconductivity in such systems [70, 89].

In 1992, Dagotto et al.[70], paid attention to the two-leg $t-J$ ladder. Using exact-diagonalization method for finite systems, they showed that the spin gap at half-filling remains finite and the pairing correlation is dominant when the carriers are doped in the two-leg $t-J$ ladder.

After the above pioneering study, a lot of works have been presented for the doped $t-J$ ladder. Density-matrix renormalization group (DMRG) calculation by Hayward et al.[96] also detects a pairing correlation decaying slightly slower than $1/r$ (r: real space distance) and a CDW correlation decaying faster than $1/r$ for an electron density of $n = 0.8$ with $J/t = 1$. Moreover, exact-diagonalization evaluation of the critical exponent is in overall agreement with the DMRG results[95, 97, 99]. Thus we can consider that the pairing correlation is dominant in the two-leg $t-J$ ladder for sufficiently large J. From an experimental point of view, the occurrence of superconductivity has indeed been reported recently in a two-leg ladder cuprate $Sr_{0.4}Ca_{13.6}Cu_{24}O_{41.84}$ [101].

On the other hand, the pairing correlation has also been studied extensively for the two-leg Hubbard ladder (Fig.1.8). From an analytical point of view, the weak-coupling theory with the bosonization combined with the renormalization-group techniques [108, 109, 110, 111] has indeed shown that the the two-leg Hubbard ladder has a spin gap and that the singlet pairing correlation function decays as $\sim r^{-1/(2K_\rho)}$ with $K_\rho = 1$ in the weak-coupling limit if the system is free from Umklapp processes, as a result of the relevant pair-tunneling process (Fig.2.1). The importance of the pair-tunneling process is reminiscent of the Suhl-Kondo mechanism for superconductivity in the two-band system.

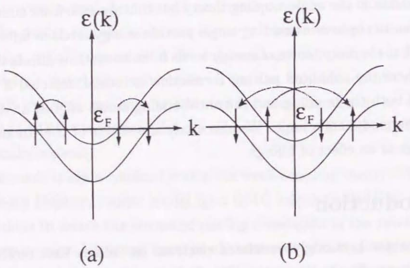

Figure 2.1: Relevant pair-tunneling processes; Fig.(a) (Fig.(b)) is the forward (backward) type pair-tunneling process.

Here K_ρ is the critical exponent for the total-charge-density mode. Since SDW and $2k_F$ CDW correlations have to decay exponentially in the presence of a spin gap in a two-leg ladder, the only phase competing with pairing correlation will be $4k_F$ CDW correlation, which should decay as r^{-2K_ρ}. Hence the pairing correlation dominates over all the others if $K_\rho > 1/2$. The exponent for the pairing correlation should be reciprocal to that of the

$4k_F$ CDW. This is called the *duality relation*[99, 110]. It is interesting that the relation still seems to hold in the $t-J$ ladder at least approximately.[96, 99]

However, the weak-coupling theory is guaranteed to be valid for infinitesimally small interaction strengths in principle. Furthermore the direct calculations for the correlation functions at the fixed point of the renormalization are only possible in the case in which the fermi velocities of both bands coincide. We have to have $U \ll t_\perp \ll t$ for this condition to be always fulfilled. Thus numerical calculations are needed to study the case of finite U and $t_\perp \sim t$, which is relevant to real systems.

In numerical calculations, however, the dominance of the pairing correlation in the Hubbard ladder appears to be a subtle problem. Namely, a DMRG study by Noack *et al.* for the doped Hubbard ladder with $n = 0.875$, $U/t = 8$, and $t_\perp = t$ (where t and $t_\perp$ are intra- and interchain hoppings, respectively) shows no enhancement of the pairing correlation over the $U = 0$ result[112, 113], while they do find an enhancement at $t_\perp = 1.5t$[113, 125]. Asai performed a quantum Monte Carlo (QMC) calculation for a 36-rung ladder with $n = 0.833$, $U/t = 2$ and $t_\perp = 1.5t$[118], in which no enhancement of the pairing correlation was found. On the other hand, Yamaji *et al.* have found an enhancement for the values of the parameters when the lowest anti-bonding band levels for $U = 0$ approach the highest occupied bonding band levels, although their results have not been conclusive due to the small system sizes (≤ 6 rungs)[117]. Thus, the existing analytical and numerical results appear to be controversial in the two-leg Hubbard ladder.

In this chapter, we[120] perform an extensive QMC calculation for the Hubbard ladder with $t_\perp \sim t$ in order to clarify the origin of the discrepancies among the existing results. We conclude that the discreteness of energy levels in finite systems affects the pairing correlation enormously.

Another point is that the above results are obtained away from special fillings where the Umklapp-scattering processes are irrelevant. Recently, Balents and Fisher[108] proposed a weak-coupling phase diagram (Fig.2.2) which displays the numbers of the gapless spin and charge phases on the $t_\perp - n$ plane (where n is the band filling). The effects of the Umklapp processes are also discussed there. At half-filling the interband Umklapp processes become relevant resulting in a spin-liquid insulator in which the pairing correlation decays exponentially. In addition, the intraband Umklapp process within the bonding band becomes relevant resulting in a gap in one charge mode in a certain parameter region where the bonding band is reduced to a half-filled band. This phase is called 'C1S2' phase because there are one gapless and two gapfull charge modes, while the phase at half-filling is called 'C0S0' phase because there is no gapless phase. We can expect that the pairing

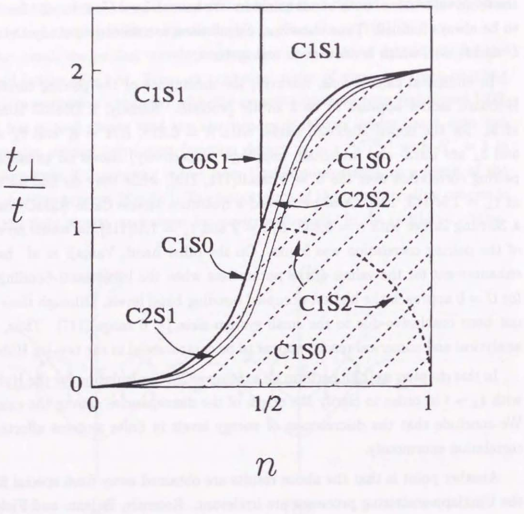

Figure 2.2: Phase diagram in the weak-coupling limit ($U \to 0$) given in ref.[108]; the numbers of the gapless charge and spin modes (x and y, respectively) are denoted as CxSy and n is the band filling. In the dark region both of the two bands cross the Fermi level.

correlation decays exponentially or is at least suppressed reflecting the existence of the charge gap, although the direct calculation of the pairing correlation has not been done. Thus we also study the effects of the Umklapp processes in this chapter, keeping in mind the above weak-coupling results.

2.2 Model and Calculation

The Hamiltonian of the two-leg Hubbard ladder is given in standard notations as

$$\begin{aligned} \mathcal{H} &= -t\sum_{\alpha i\sigma}(c^\dagger_{\alpha i\sigma}c_{\alpha i+1\sigma} + \text{h.c.}) \\ &\quad -t_\perp \sum_{i\sigma}(c^\dagger_{1,i\sigma}c_{2,i\sigma} + \text{h.c.}) + U\sum_{\alpha i} n_{\alpha i\uparrow}n_{\alpha i\downarrow}, \end{aligned} \tag{2.1}$$

where $\alpha(= 1, 2)$ specifies the chains.

In the weak-coupling theory, the amplitude of the pair hopping process across the bonding and anti-bonding bands in momentum space flows into the strong-coupling regime upon renormalization, resulting in the formation of gaps in the two spin modes and in one of the charge modes when the Umklapp processes are irrelevant. This leaves one charge mode massless, where the mode is characterized by a critical exponent K_ρ, which should be close to unity in the weak-coupling regime. Then the correlation function of an interchain singlet pairing (Fig.1.5),

$$O_i = (c_{1i\uparrow}c_{2i\downarrow} - c_{1i\downarrow}c_{2i\uparrow})/\sqrt{2}, \tag{2.2}$$

decays like $r^{-1/(2K_\rho)}$. Here, we have applied the projector quantum Monte Carlo method[28, 29, 30, 31, 32] to look into the ground state correlation function $P(r) \equiv \langle O^\dagger_{i+r}O_i\rangle$ for this pairing. We assume the periodic boundary conditions along the chain direction, $c_{N+1} \equiv c_1$, where N labels the rungs.

The details of the QMC calculation are the following. We took the non-interacting Fermi sea as the trial state. The projection imaginary time τ was taken to be $\sim 60/t$. We need such a large τ to ensure the convergence of especially the long-range part of the pairing correlation. This sharply contrasts with the situation for single chains, where $\tau \sim 20/t$ suffices for the same sample length as considered here. The large value of τ, along with a large on-site repulsion U, makes the negative-sign problem serious, so that the calculation is feasible for $U/t \leq 2$. In the Trotter decomposition, the imaginary time increment $[\tau/(\text{number of Trotter slices})]$ is taken to be ≤ 0.1. We have concentrated on band fillings for which the closed-shell condition (no degeneracy in the non-interacting Fermi sea) is met. We set $t = 1$ hereafter.

The tractable strengths of the interaction $U(\leq 2t)$ are considerably smaller than the value ($U \sim 12t$)[126, 127] estimated from the cuprates if the Hubbard model is one of the relevant models for the cuprates. However, it should be interesting to look at the Hubbard ladder with a moderate U, since it is a highly non-trivial question whether the properties of even the moderate coupling regime are connected continuously to those for the weak-coupling regime.

2.3 Detection of the Enhanced Pairing Correlation

In the beginning we show in Fig.2.3 the result for $P(r)$ for $t_\perp = 0.98$ and $t_\perp = 1.03$ with $U = 1$ and the band filling $n = 0.867 = 52$ electrons/ (30 rungs × 2 legs).

The $U = 0$ result (dashed line) for these two values of $t_\perp$ are identical because the Fermi sea remains unchanged. However, if we turn on U, the 5% change in the $t_\perp = 0.98 \rightarrow 1.03$ is enough to cause a dramatic change in the pairing correlation: for $t_\perp = 0.98$ the correlation has a large enhancement over the $U = 0$ result at large distances, while the enhancement is not seen for $t_\perp = 1.03$.

In fact we have deliberately chosen these values to control the alignment of the discrete energy levels at $U = 0$. Namely, when $t_\perp = 0.98$, the single-electron energy levels of the bonding and anti-bonding bands for $U = 0$ lie close to each other around the Fermi level with the level offset ($\Delta\varepsilon$ in the inset of Fig.2.3) being as small as 0.004, while they are staggered for $t_\perp = 1.03$ with the level offset of 0.1. On the other hand, the size of the spin gap is known to be around 0.05 for $U = 8$[125, 113], and is expected to be of the same order of magnitude or smaller for smaller values of U. The present result then suggests that if the level offset $\Delta\varepsilon$ is too large compared to the spin gap (which should be O(0.01) for $U \sim t$[113]), the enhancement of the pairing correlation is smeared. By contrast, for a small enough $\Delta\varepsilon$, by which an infinite system is mimicked, the enhancement is indeed detected in agreement with the weak-coupling theory, in which the spin gap is assumed to be infinitely large at the fixed point of the renormalization flow. In usual 3D systems, the energy to be compared with $\Delta\epsilon$ would be the BCS gap parameter, Δ_{BCS}. However, if one considers a purely 1D system, a BCS gap can be absent even when a pairing correlation is dominant, since a gapless excitation can exist as in the present case. Thus the only energy scale left is the spin gap. We also comment on the situation when the inter-ladder coupling is considered at the end of this chapter.

Our result is reminiscent of those obtained by Yamaji *et al.*[117], who found an enhancement of the pairing correlation in a restricted parameter regime where the lowest anti-bonding levels approach the highest occupied bonding levels. They conclude that the

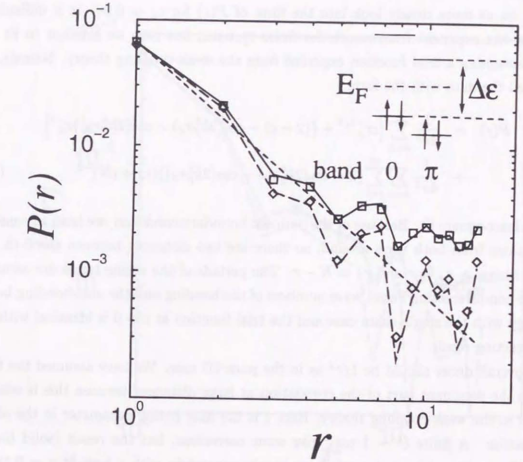

Figure 2.3: Pairing correlation function, $P(r)$, plotted against the real-space distance r in a 30-rung Hubbard ladder having 52 electrons for $U = 1$ with $t_\perp = 0.98$ (□) and $t_\perp = 1.03$ (◇). The dashed line is the non-interacting result for the same system size, while the straight dashed line represents $\propto 1/r^2$. The solid line is a fit to the $U = 1$ result with $t_\perp = 0.98$ (see text). The inset shows a schematic image of the discrete energy levels of both bonding (0) and anti-bonding (π) bands for $U = 0$.

pairing correlation is dominant when the anti-bonding band 'slightly touches' the Fermi level. However, our result in Fig.2.3 is obtained for the band filling for which no less than seven out of 30 anti-bonding levels are occupied at $U = 0$. Hence the enhancement of the pairing correlation is seen to be not restricted to the situation where the anti-bonding band edge touches the Fermi level.

Now, let us more closely look into the form of $P(r)$ for $t_\perp = 0.98$. It is difficult to determine the exponent from results for finite systems, but here we attempt to fit the data by assuming a trial function expected from the weak-coupling theory. Namely, we have fitted the data with the form,

$$\begin{aligned} P(r) &= \frac{1}{4\pi^2}\sum_{d=\pm}\left[c r_d^{-1/2} + \{(2-c) - \cos(2k_F^0 r_d) - \cos(2k_F^\pi r_d)\} r_d^{-2}\right] \\ &+ \frac{1}{4\pi^2}\sum_{d=\pm}\sum_{i=1}^{\infty}\{2 - \cos(2k_F^0 r_d) - \cos(2k_F^\pi r_d)\}(r_d + iN)^{-2} \end{aligned} \quad (2.3)$$

with the least-square fit. Because of the periodic boundary condition, we have to consider contributions from both ways around, so there are two distances between the 0-th and the r-th rung, i.e, $r_+ = r$ and $r_- = N - r$. The periods of the cosine terms are assumed to be the non-interacting Fermi wave numbers of the bonding and the anti-bonding bands in analogy with the single-chain case and the trial function at $c = 0$ is identical with the non-interacting result.

The overall decay should be $1/r^2$ as in the pure 1D case. We have assumed the form $c/r^{1/2}$ as the dominant part of the correlation at large distances because this is what is expected in the weak-coupling theory. Here c is the only fitting parameter in the above trial function. A finite $U \sim 1$ may give some correction, but the result (solid line in Fig.2.3) fits to the numerical result surprisingly accurately with a best-fit $c = 0.10$. If we least-square fit the exponent itself as $1/r^\alpha$, we have $\alpha < 0.7$ with a similar accuracy. Thus a finite U may change α, but $\alpha > 1$ may be excluded. To fit the short-range part of the data, a non-oscillating $(2 - c)/r^2$ term is required, which is not present in the weak-coupling theory. We believe that this is because the weak-coupling theory only concerns with the asymptotic form of the correlation functions.

In Fig.2.4, we show a result for a larger system size (42 rungs) for a slightly different electron density, $n = 0.905$ with 76 electrons and $t_\perp = 0.99$. We have again an excellent fit with $c = 0.07$ this time.

In Fig.2.5, we display the result for a larger $U = 2$. We again have a long-ranged $P(r)$ at large distances, although $P(r)$ is slightly reduced from the result for $U = 1$. This is consistent with the weak-coupling theory, in which K_ρ is a *decreasing* function of U so

that after the spin gap opens for $U > 0$, the pairing correlation decays faster for larger values of U.

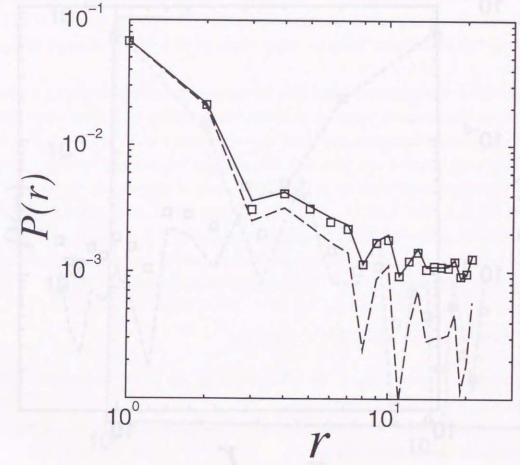

Figure 2.4: Similar plot as in Fig.2.3 for a 42-rung system having 76 electrons with $t_\perp = 0.99$.

2.4 Effects of the Umklapp Processes

Next we explore the effects of the Umklapp processes. For that purpose we concentrate on the filling dependence for a fixed interaction $U = 2$. We have tuned the value of $t_\perp$ to ensure that the level offset $(\Delta\varepsilon)$ at the Fermi level is as small as O(0.01) for $U = 0$. In

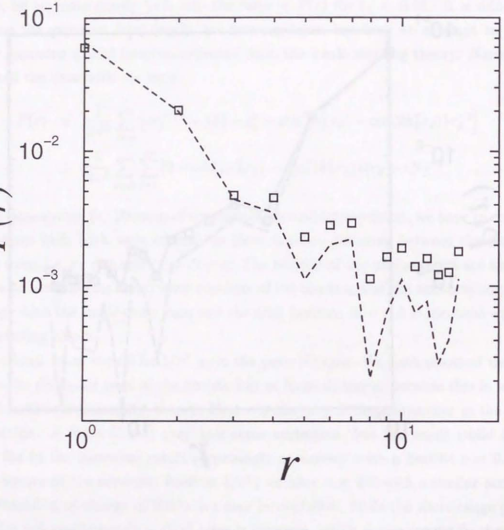

Figure 2.5: Similar plot as in Fig.2.3 except $U = 2$ here.

this way, we can single out the effects of the Umklapp processes from those due to large values of $\Delta\varepsilon$. If we first look at the half-filling (Fig.2.6), the decaying form is essentially similar to the $U = 0$ result. At half-filling, the interband Umklapp processes emerge and, according to the weak-coupling theory, open a charge gap, which results in an exponential decay of the pairing correlation. (We should note that there are two kinds of charge gaps.

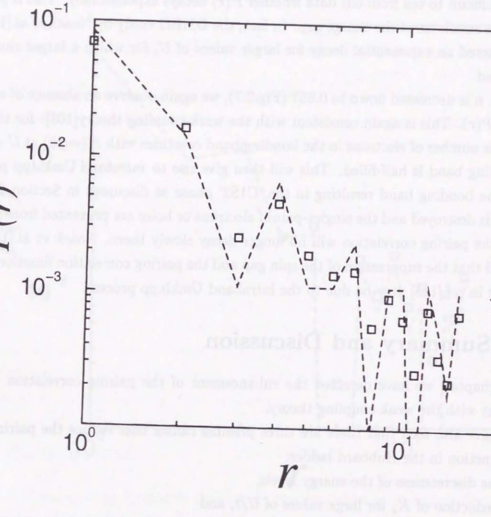

Figure 2.6: Pairing correlation $P(r)$ (□) against r for a 30-rung system for $U = 2$ with $t_\perp = 0.99$ and 60 electrons (half-filled). The dashed line represents the non-interacting result.

The one, which is produced by the pair-tunneling processes, causes the long range order of the Josephson phase resulting in the enhancement of the pairing correlation as in the previous section, while the other, which is produced by the Umklapp processes, causes the long range order of the phase of the CDW resulting in the suppression of the pairing correlation as in the present section.)

It is difficult to tell from our data whether $P(r)$ decays exponentially. This is probably due to the smallness of the charge gap. In fact, the DMRG study by Noack *et al.*[112, 113] have detected an exponential decay for larger values of U, for which a larger charge gap is expected.

When n is decreased down to 0.667 (Fig.2.7), we again observe an absence of enhancement in $P(r)$. This is again consistent with the weak-coupling theory[108]: for this band filling, the number of electrons in the bonding band coincides with $N(=30)$ at $U=0$, i.e., the bonding band is half-filled. This will then give rise to *intraband* Umklapp processes within the bonding band resulting in the 'C1S2' phase as discussed in Section 2.1. The spin gap is destroyed and the singlet-pair of electrons or holes are prevented from forming, so that the pairing correlation will no longer decay slowly there. Noack et al.[113] have suggested that the suppression of the spin gap and the pairing correlation function around $t_\perp = 0.4t$ in ref.[125] may be due to the intraband Umklapp process.

2.5 Summary and Discussion

In this chapter, we have detected the enhancement of the pairing correlation which is consistent with the weak-coupling theory.

We have also seen that there are three possible causes that reduce the pairing correlation function in the Hubbard ladder:

(i) the discreteness of the energy levels,

(ii) reduction of K_ρ for large values of U/t, and

(iii) effect of intra- and interband Umklapp processes around specific band fillings.

The discreteness of the energy levels is a finite-size effect, while the others are present in infinite systems as well. We can make a possible interpretation for the existing results in terms of these effects. For 60 electrons on 36 rungs with $t_\perp = 1.5t$ in ref.[118], for instance, the non-interacting energy levels have a significant offset $\sim 0.15t$ between bonding and anti-bonding levels at the Fermi level, which may be the reason why the pairing correlation is not enhanced for $U/t = 2$. For a large $U/t(=8)$ in ref.[112, 125, 113], (ii) and/or (iii) in the above may possibly be important in making the pairing correlation for $t_\perp = t$ not enhanced. The effect (iii) should be more serious for $t_\perp = t$ than for $t_\perp = 1.5t$ because the

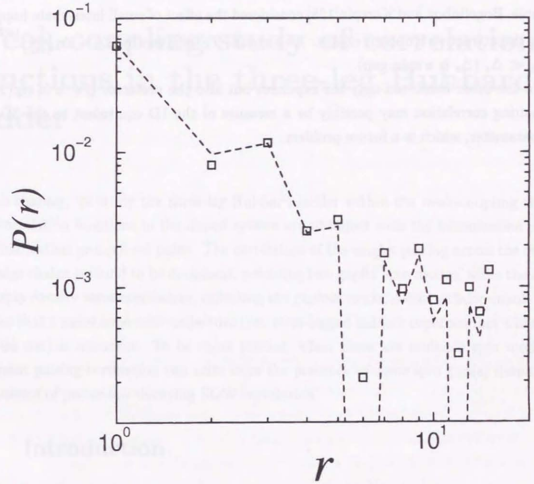

Figure 2.7: Pairing correlation $P(r)$ (□) against r for a 30-rung system for $U=2$ with $t_\perp = 1.01$ and 40 electrons (half-filled bonding band). The dashed line represents the non-interacting result.

bonding band is closer to the half-filling in the former. On the other hand, the discreteness of the energy levels might exert some effects as well, since the non-interacting energy levels for a 32-rung ladder with 56 electrons ($n = 0.875$) in an open boundary condition have an offset of $0.15t$ at the Fermi level for $t_\perp = t$ while the offset is $0.03t$ for $t_\perp = 1.5t$.

In a real system, the inter-ladder couplings should exist, so that the system is 3D. In this case, we can indeed expect a finite superconducting transition temperature T_C. For example, Bogoliubov and Korepin[128] considered the effect of small inter-chain hoppings, $t_{\rm in}$ on the attractive Hubbard chains. As a result, T_C is given by $T_C \sim \Delta_s\left(\frac{t_{\rm in}}{\Delta_s}\right)^{1/(2-K_\rho^{-1})}$ for $t_{\rm in} \ll \Delta_s$ (Δ_s is a spin gap).

On the other hand, not only the exponent but also the prefactor (i.e. c in eq.(2.3) of the pairing correlation may possibly be a measure of the 1D equivalent to the 3D BCS gap parameter, which is a future problem.

Chapter 3

Weak-coupling study of correlation functions in the three-leg Hubbard ladder

In this chapter, we study the three-leg Hubbard ladder within the weak-coupling theory. The correlation functions in the doped system are obtained with the bosonization at the renormalization-group fixed point. The correlation of the singlet pairing across the central and edge chains is found to be dominant, reflecting two gapful spin modes, while the intra-edge spin density wave correlation, reflecting the gapless mode, is only subdominant. This implies that a naive even-odd conjecture (i.e. even-legged ladders superconduct while odd ones do not) is incorrect. To be more precise, when there are multiple spin modes, a dominant pairing correlation can arise from the presence of *some* spin gap(s) despite the coexistence of power-law decaying SDW correlation.

3.1 Introduction

As stated in Chapter 1, an increasing fascination toward ladder systems has been kicked off by an 'even-odd' conjecture by Schulz[65] and independently by Rice et al.[89], who have proposed that the ladder, at half-filling, with even number of chains should be a spin liquid reflecting the absence of gapless spin excitations, while odd-numbered chains should be antiferromagnetic (AF) reflecting the presence of gapless spin excitations [70, 71, 72, 73, 74, 75, 76, 77, 78, 79, 80]. This is reminiscent of Haldane's conjecture [65, 66, 67, 68] for the 1D AF Heisenberg model for integer and half-odd-integer spins. Experimentally, cuprates $SrCu_2O_3$ and $Sr_2Cu_3O_5$ are investigated as prototypes of two- and three-leg systems, respectively. The two-leg system ($SrCu_2O_3$) indeed shows a spin-liquid behavior characteristic of a finite SDW length, while the three-leg system ($Sr_2Cu_3O_5$) shows an AF behavior[83, 84, 85, 86, 87]. When the system is doped with carriers, it is usually supposed that an even-numbered ladder should exhibit superconductivity with the interchain singlet pairing as expected from the persistent spin gap, while an odd-numbered ladder should have the usual $2k_F$ SDW reflecting the gapless spin excitations. In the two-leg case, intensive analytical and numerical studies have been performed as discussed in Chapter 1 and Chapter 2. If we give a summary of the results, the dominance of the pairing correlation in the $t-J$ ladder is confirmed in a certain parameter region wider than that of the single chain case. Furthermore, the dominance of the pairing correlation in the Hubbard ladder is also shown in the weak-coupling limit and the enhancement of the pairing correlation is confirmed even for intermediate U as shown in Chapter 2.

Theoretically, however, whether the 'even-odd' conjecture continues to be valid for triple chains remains an open question. There had been no results for the pairing correlation function in the three-leg $t-J$ or Hubbard ladder (Fig.1.9).

On the other hand, Arrigoni has looked into a three-leg with weak Hubbard-type interactions by the usual perturbational renormalization-group technique, which is quite similar to that developed by Balents and Fisher for the two-leg case[108], to conclude that gapless and gapful spin excitations *coexist* there[122].

Namely, he has actually enumerated the numbers of gapless charge and spin modes on the phase diagram spanned by the doping level and the interchain hopping. He found that, at half-filling, one gapless spin mode exists for the interchain hopping comparable with the intrachain hopping, in agreement with some experimental results and theoretical expectations (Fig.3.1). Away from the half-filling, on the other hand, one gapless spin mode is found to remain at the fixed point in the region where the fermi level intersects all the three bands in the noninteracting case. From this, Arrigoni argues that the $2k_F$ SDW correlation should decay as a power law as expected from experiments.

On the other hand, his result also indicates that two gapful spin modes exist in addition. While a spin gap certainly favors a singlet superconducting (SS) correlation when there is only one spin mode, we are in fact faced here with an intriguing problem of what happens when gapless and gapful spin modes coexist, since it may well be possible that the presence of gap(s) in *some* out of multiple spin modes may be sufficient for the dominance of a paring correlation. Furthermore, as discussed below, the gaps of two spin modes emerge as an effect of the *pair-tunneling process* across the top and the bottom bands (Fig.3.2). This is reminiscent of the two-leg case and of the Suhl-Kondo mechanism [114, 115]. These have motivated us, in this chapter, to actually look at the correlation functions using the bosonization method[51, 52] at the fixed point away from half-filling.

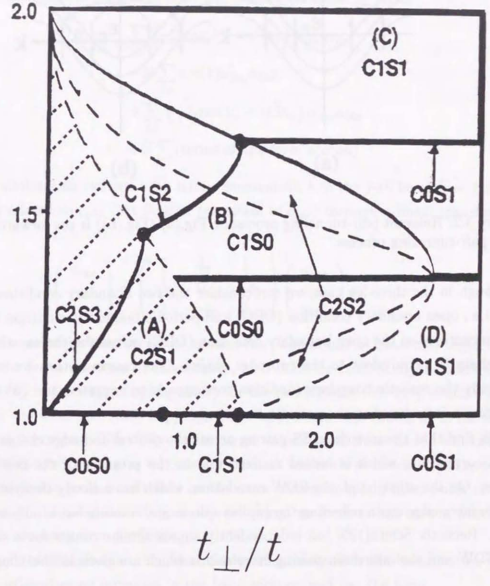

Figure 3.1: Phase diagram in the weak-coupling limit ($U \to 0$) given in ref.[122]; where the numbers of the gapless charge and spin modes (x and y, respectively) are denoted as CxSy and $\rho \equiv 2-n$ (n is the band filling). In the dark region all the three bands cross the Fermi level.

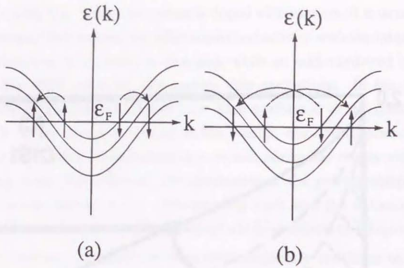

Figure 3.2: Relevant pair-tunneling processes; Fig.(a) (Fig.(b)) is the forward (backward) type pair-tunneling process.

Although in the three-leg case, we can consider the two boundary conditions across the legs, i.e., open boundary condition (OBC) and periodic boundary condition (PBC), here we concentrate on the open boundary condition (OBC) across the chains, where the central chain is inequivalent to the two edge chains. The reason is that we would like to (i) study the realistic boundary condition corresponds to cuprates, and (ii) to avoid the frustration introduced in the periodic three-legs.

We find that the interchain SS pairing across the central and edge chains is the dominant correlation, which is indeed realized due to the presence of the two gapful spin modes. On the other hand, the SDW correlation, which has a slowly-decaying power law for the intra-edge chain reflecting the gapless spin mode, coexists but is only subdominant [121]. Recently Schulz[123] has independently shown similar results for a subdominant $2k_F$ SDW and the interchain pairing correlations which are given in this chapter.

3.2 Model and the Calculation

The three-leg Hubbard model with OBC is defined by the following Hamiltonian,

$$\begin{aligned} H = & -t\sum_{\mu i\sigma}(c^\dagger_{\mu i\sigma}c_{\mu i+1\sigma} + \text{h.c.}) \\ & -t_\perp \sum_{i\sigma}(c^\dagger_{\alpha i\sigma}c_{\beta i\sigma} + c^\dagger_{\beta i\sigma}c_{\gamma i\sigma} + \text{h.c.}) \end{aligned}$$

$$+U\sum_{\mu i} n_{\mu i\uparrow}n_{\mu i\downarrow}, \tag{3.1}$$

where $t(t_\perp)$ is the intra-(inter-)chain hopping, i labels the rung while $\mu = \alpha, \beta, \gamma$ labels the leg (with β being the central one). In the momentum space we have

$$\begin{aligned} H = & \sum_{k\sigma}\left(-2t\cos(k) - \sqrt{2}t_\perp\right) a^\dagger_{1k\sigma}a_{1k\sigma} \\ & -2t\sum_{k\sigma}\cos(k)a^\dagger_{2k\sigma}a_{2k\sigma} \\ & +\sum_{k\sigma}\left(-2t\cos(k) + \sqrt{2}t_\perp\right) a^\dagger_{3k\sigma}a_{3k\sigma} \\ & +U\sum(\text{terms of the form } a^\dagger a^\dagger aa). \end{aligned} \tag{3.2}$$

Here $a_{jk\sigma}$ annihilates an electron with lattice momentum k in the j-th band ($j = 1, 2, 3$), where $a_{jk\sigma}$ is related to $c_{\mu k\sigma}$ (the Fourier transform of $c_{\mu i\sigma}$) through a linear transformation,

$$\begin{pmatrix} c_{\alpha k\sigma} \\ c_{\beta k\sigma} \\ c_{\gamma k\sigma} \end{pmatrix} = \begin{pmatrix} \frac{1}{2} & \frac{1}{\sqrt{2}} & \frac{1}{2} \\ \frac{1}{\sqrt{2}} & 0 & -\frac{1}{\sqrt{2}} \\ \frac{1}{2} & -\frac{1}{\sqrt{2}} & \frac{1}{2} \end{pmatrix} \begin{pmatrix} a_{1k\sigma} \\ a_{2k\sigma} \\ a_{3k\sigma} \end{pmatrix}. \tag{3.3}$$

Hereafter we linearize the band structure around the fermi points as usual and neglect the difference in the fermi velocities of three bands, as is done for calculating the correlation functions directly in the weak-coupling theory for the two-leg case[109, 111], which will be acceptable for the weak interchain hopping. These approximations enable us to calculate the correlation functions. The difference in fermi velocities of three bands will not be important qualitatively as long as we consider the case where three bands cross the fermi energy, for which Arrigoni's result falls on the same strong coupling fixed point on the plane of interchain hopping and filling. In the following, we focus on the case in which all of three bands are away from half-filling.

The part of the Hamiltonian, H_d, that can be diagonalized in the bosonization only includes forward-scattering processes in the band picture, and has the form

$$\begin{aligned} H_\text{d} &= H_\text{spin} + H_\text{charge}, \\ H_\text{spin} &= \sum_i \frac{v_{\sigma i}}{4\pi}\int dx[\frac{1}{K_{\sigma i}}(\partial_x\phi_{i+})^2 + K_{\sigma i}(\partial_x\phi_{i-})^2], \\ H_\text{charge} &= \sum_i \frac{v_{\rho i}}{4\pi}\int dx[\frac{1}{K_{\rho i}}(\partial_x\chi_{i+})^2 + K_{\rho i}(\partial_x\chi_{i-})^2]. \end{aligned} \tag{3.4}$$

Here ϕ_{i+} is the spin phase field of the i-th band, χ_{i+} is the diagonal charge phase field, while $\phi_{i-}(\chi_{i-})$ is the field dual to $\phi_{i+}(\chi_{i+})$, $K_{\sigma i}(K_{\rho i})$ the correlation exponent for the

$\phi(\chi_i)$ phase with $v_{\sigma i}(v_{\rho i})$ being their velocities. For the Hubbard-type interaction, we have $v_{\sigma i} = v_F$, $K_{\sigma i}$=1 for all i's, while $v_{\rho 1} = v_F$, $v_{\rho 2} = v_F\sqrt{1-4g^2}$, $v_{\rho 3} = v_F\sqrt{1-g^2/4}$, $K_{\rho 1} = 1$, $K_{\rho 2} = \sqrt{(1-2g)/(1+2g)}$, $K_{\rho 3} = \sqrt{(1-g/2)/(1+g/2)}$, where $g = U/2\pi v_F$ is the dimensionless coupling constant. The derivation of the above equation is given in the Appendix.

The diagonalized charge field $\chi_{i\pm}$ is linearly related to the initial charge field $\theta_{i\pm}$ of the i-th band as

$$\begin{pmatrix} \theta_{1\pm} \\ \theta_{2\pm} \\ \theta_{3\pm} \end{pmatrix} = \begin{pmatrix} \frac{1}{\sqrt{2}} & \frac{1}{\sqrt{3}} & \frac{1}{\sqrt{6}} \\ 0 & \frac{1}{\sqrt{3}} & -\sqrt{\frac{2}{3}} \\ -\frac{1}{\sqrt{2}} & \frac{1}{\sqrt{3}} & \frac{1}{\sqrt{6}} \end{pmatrix} \begin{pmatrix} \chi_{1\pm} \\ \chi_{2\pm} \\ \chi_{3\pm} \end{pmatrix}, \tag{3.5}$$

where both $\theta_{i\pm}$ and $\phi_{\pm}$ are related to the field operator for electrons $\psi_{i+(-)\sigma}$, which annihilates an electron on the right-(left-) going branch in band i as

$$\begin{aligned} \psi_{i+(-)\sigma}(x) &= \frac{\eta_{i+(-)\sigma}}{2\pi\Lambda}\exp\{\pm ik_{iF}x \\ &\pm\frac{i}{2}[\theta_{i+}(x) \pm \theta_{i-}(x) + \sigma(\phi_{i+}(x) \pm \phi_{i-}(x))]\}. \end{aligned} \tag{3.6}$$

Here the $\eta_{ir\sigma}$'s are Haldane's U operators [55, 56] which ensure the anti-commutation relations between electron operators through the relation, $\{\eta_{ir\sigma}, \eta_{i'r'\sigma'}\}_+ = 2\delta_{ii'}\delta_{rr'}\delta_{\sigma\sigma'}$, $\eta^\dagger_{ir\sigma} = \eta_{ir\sigma}$.

There are still many scattering processes corresponding to both the backward and the pair-tunneling scattering processes, which cannot be treated exactly. Arrigoni examined the effect of such scattering processes by the perturbational renormalization-group technique. He found that the backward-scattering interaction within the first or the third band turn from positive to negative as the renormalization is performed and that the pair-tunneling processes across the first and third bands also become relevant. As far as the relevant scattering processes are concerned, the first (third) band plays the role of the bonding (anti-bonding) band in the two-leg case. At the fixed point the Hamiltonian density, H^*, then takes the form, in term of the phase variables,

$$\begin{aligned} H^* &= -\frac{g_b(1)}{\pi^2\Lambda^2}\cos(2\phi_{1+}(x)) - \frac{g_b(3)}{\pi^2\Lambda^2}\cos(2\phi_{3+}(x)) \\ &+\frac{2g_{ft}(1,3)}{\pi^2\Lambda^2}\cos(\sqrt{2}\chi_{1-}(x))\sin\phi_{1+}(x)\sin\phi_{3+}(x), \end{aligned} \tag{3.7}$$

where both $g_b(1)$ and $g_b(3)$ are negative large quantities, and $g_{ft}(1,3)$ is a positive large quantity.

This indicates that the phase fields ϕ_{1+}, ϕ_{3+}, and χ_{1-} are long-range ordered and fixed at $\pi/2$, $\pi/2$, and $\pi/\sqrt{2}$, respectively, which in turn implies that the correlation functions

that contain ϕ_{1-}, ϕ_{3-}, and χ_{1+} fields decay exponentially. The renormalization procedure will affect the velocities and the critical exponents for the gapless fields, $\chi_{2\pm}$, $\chi_{3\pm}$, and $\phi_{2\pm}$, so that we should end up with renormalized v^*'s and K^*'s.

In principle, the numerical values of renormalized v^*'s and K^*'s for finite g may be obtained from the renormalization equations as has been attempted for a double chain by Balents and Fisher [108], although it would be difficult in practice. However, at least in the weak-coupling limit, $g \to 0$, to which our treatment is meant to fall upon, we shall certainly have $v^* \simeq v_F$ and $K^* \simeq 1$ for *gapless* modes even after the renormalization procedure.

3.3 Results for the Correlation Functions

Now we are in position to calculate the correlation functions, since the gapless fields have already been diagonalized, while the remaining gapful fields have the respective expectation values. The details of the calculation of the correlation functions are given in the Appendix. The two-particle correlation functions which include the following two particle operators in the band description are shown to have a power-law decay:

(1) operators constructed from two operators involving only the second band (since the charge and the spin phases are both gapless, electrons in this band should have the usual TL-liquid behavior),

(2) order parameters of singlet superconductivity within the first or third band, $\psi_{1+\uparrow(\downarrow)}\psi_{1-\downarrow(\uparrow)}$, $\psi_{3+\uparrow(\downarrow)}\psi_{3-\downarrow(\uparrow)}$.

As a result, the order parameters that possess power-law decays should be the following,

(A) The correlations within each of the two edge (α and γ) chains or across the two edge chains:

(a) $2k_F$ CDW,
$O_{\text{intra}2k_F\text{CDW}} = \psi^\dagger_{\alpha(\gamma)+\uparrow}\psi_{\alpha(\gamma)-\uparrow}$; $O_{\text{interCDW}} = \psi^\dagger_{\alpha(\gamma)+\uparrow}\psi_{\gamma(\alpha)-\uparrow}$,

(b) $2k_F$ SDW,
$O_{\text{intraSDW}} = \psi^\dagger_{\alpha(\gamma)+\uparrow}\psi_{\alpha(\gamma)-\downarrow}$; $O_{\text{interSDW}} = \psi^\dagger_{\alpha(\gamma)+\uparrow}\psi_{\gamma(\alpha)-\downarrow}$,

(c) singlet pairing (SS),
$O_{\text{intraSS}} = \psi_{\alpha(\gamma)+\uparrow}\psi_{\alpha(\gamma)-\downarrow}$; $O_{\text{interSS}} = \psi_{\alpha(\gamma)+\uparrow}\psi_{\gamma(\alpha)-\downarrow}$,

(d) triplet pairing (TS),
$O_{\text{intraTS}} = \psi_{\alpha(\gamma)+\uparrow}\psi_{\alpha(\gamma)-\uparrow}$; $O_{\text{interTS}} = \psi_{\alpha(\gamma)+\uparrow}\psi_{\gamma(\alpha)-\uparrow}$,

(B) The $4k_F$ CDW which is written with four electron operators,
$O_{4k_F\text{CDW}} = \psi^\dagger_{\nu+\uparrow}\psi^\dagger_{\nu+\downarrow}\psi_{\nu-\uparrow}\psi_{\nu-\downarrow}$ $(\nu = \alpha, \beta, \gamma)$,

(C) The singlet pairing across the *central* chain (β) and edge chains (Fig.3.3),

$O_{\rm CESS} = \sum_\sigma \sigma(\psi_{\alpha+\sigma} + \psi_{\gamma+\sigma})\psi_{\beta-,-\sigma}$.
In the band picture we can rewright $O_{\rm CESS}$ as comprising

$$O_{\rm CESS} \sim \sum_\sigma \sigma(\psi_{1+\sigma}\psi_{1-,-\sigma} - \psi_{3+\sigma}\psi_{3-,-\sigma}). \tag{3.8}$$

We cannot easily name the symmetry of the pairing, although we naively might call this pairing d-wave-like in a similar sense as in the two-leg case, in which a pair is called d-wave when the pairing, in addition to being off-site, consists of a bonding band and an anti-bonding band pairs with opposite signs[108, 109, 110, 111, 113]. Thus the edge-

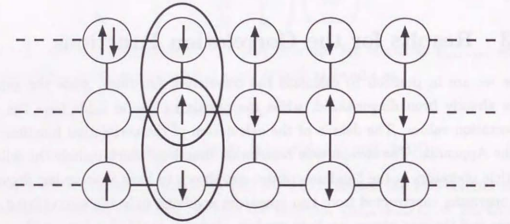

Figure 3.3: Schematic picture for the interchain (CESS) pairing in the doped three-leg Hubbard ladder.

chain SDW correlation has a power-law decay, while the SDW correlation within the central chain decays exponentially since it consists of the terms containing ϕ_{1-} and/or ϕ_{3-} phases. Although we consider the case away from half-filling, the SDW correlation should obviously be more enhanced at half-filling. The experiments at half-filling do not contradict the present results, since the experiments should detect the total SDW correlation of all the chains and the SDW correlation is more enhanced at half-filling. However the present theory corresponds only to the infinitesimally small interaction in principle, although the actual cuprates have a strong interactions between electrons.

Intra- or inter-edge correlation functions have to involve forms bilinear in $a_{2k\sigma}$ in eq.(3.3). They are described in terms of the charge field θ_2 for the second band, which does not contain χ_1, a phase-fixed field (see eq.(3.5)). Thus the edge-channel correlations are completely determined by the character of the second band (the Luttinger-liquid band), while the other phase fields, being gapful, are irrelevant. The final result for the edge-channel correlations at large distances, up to $2k_F$ oscillations, is as follows regardless

of whether the correlation is intra- or inter-edge:

$$\begin{aligned}
\langle O_{2k_F{\rm CDW}}(x)O^\dagger_{2k_F{\rm CDW}}(0)\rangle &\sim x^{-\frac{1}{3}(K^*_{\rho2}+2K^*_{\rho3})-1}, \\
\langle O_{\rm SDW}(x)O^\dagger_{\rm SDW}(0)\rangle &\sim x^{-\frac{1}{3}(K^*_{\rho2}+2K^*_{\rho3})-1}, \\
\langle O_{\rm SS}(x)O^\dagger_{\rm SS}(0)\rangle &\sim x^{-\frac{1}{3}(\frac{1}{K^*_{\rho2}}+\frac{2}{K^*_{\rho3}})-1}, \\
\langle O_{\rm TS}(x)O^\dagger_{\rm TS}(0)\rangle &\sim x^{-\frac{1}{3}(\frac{1}{K^*_{\rho2}}+\frac{2}{K^*_{\rho3}})-1}.
\end{aligned} \tag{3.9}$$

(where we have put $K^*_\sigma = 1$ for the present spin-independent interaction.[123]) In addition, the $4k_F$ CDW correlation decays as

$$\langle O_{4k_F{\rm CDW}}(x)O^\dagger_{4k_F{\rm CDW}}(0)\rangle \sim x^{-\frac{2}{3}(2K^*_{\rho2}+K^*_{\rho3})}. \tag{3.10}$$

By contrast, if we look at the pairing $O_{\rm CESS}(x)$ across the central chain and the edge chains, this pairing, which circumvents the on-site repulsion and is linked by the resonating valence bonding across the neighboring chains, is expected to be stronger than other correlations as in the two-leg case. The correlation function for $O_{\rm CESS}(x)$ is indeed calculated to be

$$\langle O_{\rm CESS}(x)O^\dagger_{\rm CESS}(0)\rangle \sim x^{-\frac{1}{3}(\frac{1}{K^*_{\rho2}}+\frac{1}{2K^*_{\rho3}})}. \tag{3.11}$$

From the calculations given in the Appendix, we can see that the interchain pairing exploits the charge gap and the spin gaps to reduce the exponent of the correlation function, in contrast to the intra-leg pairing. In addition to that, we also find that the roles of the first (third) band corresponds to those of the bonding (anti-bonding) band in the two-leg case, as far as the dominant pairing correlation is concerned. If we consider the weak-interaction limit ($U \to +0$) as in the two-leg case, all the K^*'s will tend to unity, where the CESS correlation decays as $x^{-1/2}$ while those of other correlations decays as x^{-2} at long distances. Thus, at least in this limit, the CESS correlation dominates over the others. The duality (which dictates that the pairing and density-wave exponents are reciprocal of each other[110]) is similar to that in the two-chain case, in which the interchain SS decays as $x^{-1/2}$ while that of the $4k_F$ CDW decays as x^{-2}.

3.4 Summary

In this Chapter, we have studied correlation functions using the bosonization method at the renormalization-group fixed point, which was obtained by Arrigoni, away from half-filling in the region where the fermi level intersects all the three bands in the non-interacting case. One gapless spin mode is found to remain at the fixed point, while two gapless spin modes are also found. Thus the gapless and the gapful spin modes coexist in this case. The existence of the gapless spin mode seems to ensure the power law decay of the $2k_F$ SDW as discussed by Arrigoni. On the other hand, the gaps on the two spin modes and one charge modes are caused by the pair-tunneling process across the two bands. This is reminiscent of the two-leg case, in which the pair-tunneling mechanism plays a central role for the dominance of the pairing correlation at least in the weak-coupling regime.

We found in this Chapter that the interchain singlet pairing *across* the central chain and either of the edge chains is the dominant correlation, while the SDW correlations in two edge chains coexist but are subdominant. The power law decay of the SDW correlation does not contradict with the even-odd conjecture at the half-filling, where the Umklapp scattering play a important role resulting in an enhancement of the SDW correlation. Schulz[123] has independently shown similar results for a subdominant SDW and the dominant pairing correlations.

The renormalization study is valid only for infinitesimally small interaction strengths and sufficiently small interchain hoppings in principle, while the actual cuprates have strong interactions between electrons, so that the relevance of the present results to the real materials is uncertain. However the present study suggests an important theoretical message that the dominance of superconductivity only requires the existence of gap(s) in *some* spin modes when there are multiple modes in multi-leg ladder systems no matter whether the number of legs is odd or even.

Chapter 4

QMC study of the pairing correlation in the three-leg Hubbard ladder

In this chapter, we look into the pairing correlation in the three-leg Hubbard ladder with the quantum Monte Carlo method similar to that used in the two-leg case in Chapter 2. The enhanced correlation for the pairing across the central and edge chains, which has been expected in the weak-coupling theory in Chapter 3 as an effect of the coexistence of gapful and gapless spin modes, is here shown to persist for intermediate interaction strengths. We also study the effects of the Umklapp processes at special fillings to probe the dependence on the band fillings.

4.1 Introduction

In the previous chapter, we have discussed the correlation functions in the three-leg Hubbard ladder within the weak-coupling theory. A key point in the previous chapter is that gapless and gapful spin excitations coexist in a three-leg ladder and the modes give rise to a peculiar situation where a specific pairing *across* the central and edge chains (that may be roughly a d-wave pairing) is dominant, while the $2k_F$ SDW on the edge chains simultaneously shows a subdominant but still long-tailed (power-law) decay associated with the gapless spin mode. In other words, the dominant pairing correlation only requires the existence of gap(s) in not all but *some* of the spin modes when there are multiple of them. This result serves as a counter-example of a naive even-odd conjecture that in the doped system, 'the pairing correlation becomes dominant in even-leg ladders with the persistent spin gap while the $2k_F$ SDW is dominant in odd-leg ladders without a spin gap'. As for the SDW, the power-law decay of the $2k_F$ SDW in doped systems suggests that the SDW correlation will decay even more slowly at half-filling where Umklapp processes should enhance the SDW. This does not contradict the experiments [83, 84, 85, 86, 87]. in which an AF correlation is detected at half-filling.

However, there is a serious question about these weak-coupling results as discussed in the two-leg case in Chapter 2. First, only for infinitesimally small interactions and sufficiently small hoppings are the results in Chapter 3 guaranteed to be valid in principle. Furthermore, when there is a gap in the excitation, the renormalization flows into a strong-coupling regime, so that the weak-coupling theory might break down even for small U. Hence it is imperative to study the problem from an independent numerical method for an intermediate strength of the Hubbard $U \sim t$ and an interchain hopping $t_\perp \sim t$. Although such a comparison of the numerical result for $U \sim t$ with the weak-coupling theory has been done for the two-leg system in Chapter 2, this does not necessarily serve to enlighten the situation in the three-leg case, where gapless and gapful modes coexist. This is exactly our motivation for the present study, which describes an extensive QMC calculation for the three-leg Hubbard ladder. In this chapter, it is shown that the QMC result indeed turns out to exhibit an enhancement of the pairing correlation even for finite coupling constants, $U/t = 1 \sim 2$[124].

In addition, we also study the effects of various Umklapp processes at special fillings as in the two-leg case keeping in mind the above Arrigoni's work[122] which also studied the effects of some Umklapp processes with the weak-coupling theory.

Throughout this chapter, we concentrate on the case in which all three bands cross the Fermi surface to explore the properties of a three-band system.

4.2 Detection of the Enhanced Pairing Correlation

In the beginning we recapitulate the weak-coupling theory in Chapter 3. [121, 123, 122], The pair-tunneling process ($a^\dagger_{1\uparrow}a^\dagger_{1\downarrow}a_{3\downarrow}a_{3\uparrow}$+h.c.) across the first and the third bands and the backward-scattering process within the first or the third band are relevant scattering processes. As a result, both two spin and one charge mode become gapful. This leaves one spin mode and two charge modes gapless, where the modes are characterized by the critical exponents, $K^*_{\sigma 2}$(= 1 for the spin independent interaction) and $K^*_{\rho 2}$, $K^*_{\rho 3}$, respectively[121]. We can recognize that the first (third) band is analogous to the bonding (anti-bonding) band in the two-leg ladder, while the second band is analogous to the single-band (Luttinger-liquid like) system.

The correlation of the intraband singlet pairing within the first or the third band, $\sum_\sigma \sigma(a_{1k\sigma}a_{1-k-\sigma} - a_{3k\sigma}a_{3-k-\sigma})$, decays like $r^{-(1/K^*_{\rho 2}+1/2K^*_{\rho 3})/3}$ at large distances. This pair,

when expressed in real space via the inverse-Fourier transform, is an interchain singlet pair across the central and edge chains, $O_i = (c_{\alpha i\sigma}+c_{\gamma i\sigma})c_{\beta i-\sigma} - (c_{\alpha i-\sigma}+c_{\gamma i-\sigma})c_{\beta i\sigma}$. All the K^*_ρ's should tend to unity in the weak-interaction limit ($U \to +0$), where the interchain pairing correlation decays as $r^{-1/2}$, while those of subdominant density-wave correlations decay as r^{-2}[121, 123]. Thus the pairing correlation is identified as the most dominant. In the weak-coupling renormalization, however, we have to make a reasoning: 'the pair-tunneling and the backward-scattering processes flow, in the weak-coupling renormalization, into the strong-coupling regime upon our integrating out the high-energy modes, which results in the formation of gaps.' Thus the validity of the weak-coupling scheme has to be tested especially when gapful and gapless modes coexist as stressed above.

Here we employ the projector Monte Carlo method [28, 29, 30, 31, 32] to look into the ground-state pairing correlation function $P(r) \equiv \langle O^\dagger_j O_{j+r}\rangle$. We assume the periodic boundary condition along the chain direction, $c_{N+1} \equiv c_1$, where N is the number of rungs. We only consider here the case where the intra- and the inter-band Umklapp processes are irrelevant because that is where the above-mentioned weak-coupling theory is valid. The details of the QMC calculation are similar to those for our QMC study for the two-leg case.[120] Specifically, the negative-sign problem makes the QMC calculation feasible for $U \leq 2t$. We set $t = 1$ hereafter.

In the two-leg case with a finite U, we have found an interesting property for finite systems: the pairing correlation is enhanced in agreement with the weak-coupling theory only when the single-electron energy levels of the bonding and the anti-bonding bands lie close to each other around the Fermi level (which is certainly the case with an infinite system).[120] When the levels are misaligned (for which a 5% change in $t_\perp$ is enough), the enhancement of the pairing correlation dramatically vanishes. In the weak-coupling theory, the ratio of the spin gap to the level offset is assumed to be infinitely large at the fixed point of the renormalization flow, so that the spin gap should naturally be detectable in finite systems only when the level offset is smaller than the gap.

We have found that this applies to the three-leg ladder as well, i.e., the pairing correlation is enhanced when the single-electron levels of the first and third bands lie close to each other. Hence we concentrate on such cases hereafter.

In the beginning we show in Fig.4.1 the result for $P(r)$ for $t_\perp = 0.92$ with $U = 1$ with the band filling $n = 0.843 = 86$ electrons/(34 rungs$\times$ 3 sites). For this choice of $t_\perp$ the levels in the first and the third bands lie close to each other around the Fermi level within 0.01. We can see that a large enhancement over the $U = 0$ result at large distances indeed exists. This is the key result of this chapter.

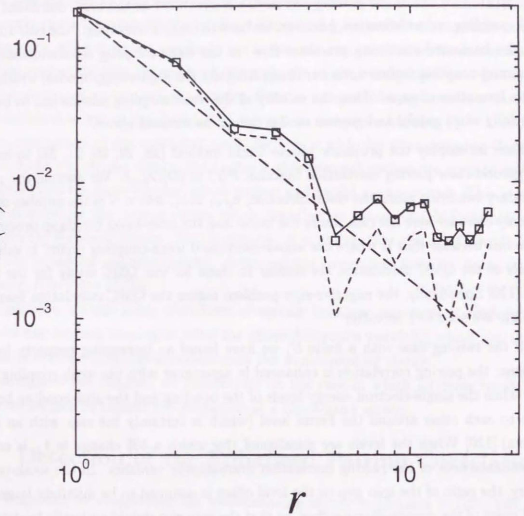

Figure 4.1: QMC result for the pairing correlation function, $P(r)(\square)$, plotted against the real space distance r in a three-leg Hubbard ladder with 34-rung having 86 electrons for $U=1$ with $t_\perp = 0.92$. The dashed line is the non-interacting result for the same system size, while the straight dashed line represents $\sim r^{-2}$. The solid line is a fit to a trial function (see text).

Although it is difficult to determine the decay exponent of $P(r)$, we can fit the data by supposing a trial function as expected from the weak-coupling theory as we did in the two-leg case [120],

$$\begin{aligned} P(r) &= \frac{1}{\pi^2}\sum_{d=\pm}\left[c r_d^{-1/2} + \{(2-c) - \cos(2k_{F1}r_d) - \cos(2k_{F3}r_d)\} r_d^{-2}\right] \\ &+ \frac{1}{\pi^2}\sum_{d=\pm}\sum_{i=1}^{\infty}\{2 - \cos(2k_{F1}r_d) - \cos(2k_{F3}r_d)\}(r_d + iN)^{-2} \end{aligned} \quad (4.1)$$

Here $k_{F1}(k_{F3})$ is the non-interacting Fermi wave number of the first (third) band, while a constant c, which should vanish for $U=0$, is here least-square fit (by taking logarithm of the data) as $c = 0.05$. As in the two-leg case, since we assume the periodic boundary condition, we have to consider contributions from both ways around, so there are two distances between the 0-th and the r-th rung, i.e., $r_+ = r$ and $r_- = N - r$. The overall decay should be $1/r^2$ as in the single-chain case, while the term $c/r^{1/2}$, the dominant correlation at large distances, is borrowed from the weak-coupling result.[121, 123] The QMC result for a finite $U = 1$ fits to the trial form (solid line in Fig.4.1) surprisingly accurately. A finite U may give some corrections to these functional forms, but even when we best-fit the exponent itself as c/r^α in place of $c/r^{1/2}$, we obtain $\alpha < 0.7$ with a similar accuracy.

In Fig.4.2, we show the result for a larger interaction $U = 2$. The result again shows an enhanced pairing correlation at large distances. However, the enhancement is slightly reduced than that in the $U = 1$ case. This is consistent with the weak-coupling theory, in which K_ρ^*'s should decrease with U.

Furthermore, we study if the presence of the second band around E_F can be detrimental to superconductivity. In Fig.4.3, we make the single-electron energy levels of all the three bands lie close to each other around the Fermi level. This is accomplished here for $t_\perp = 0.685$ and the band filling $n = 0.719 = 82$ electrons/(38 rungs $\times$ 3 sites). The highest occupied level of the second band then lies between that of the first band and the lowest unoccupied level of the third band (lying above the highest occupied level of the first band by as small as 0.01, inset of Fig.4.3).

The result in Fig.4.3 for $U = 1$ shows that the pairing correlation is enhanced as well. Thus we may consider that the second band does not hinder the enhancement of the pairing correlation in other bands. This is also consistent with the weak-coupling theory, in which all of the scattering processes connected with the second band are irrelevant. The fit of the correlation function to the trial one is again excellent with $c = 0.03$.

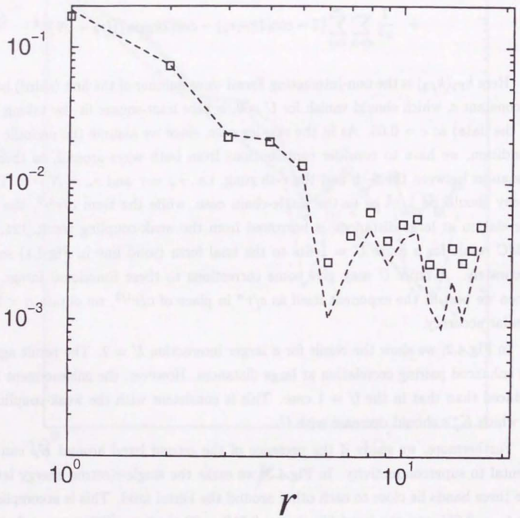

Figure 4.2: Similar plot as in Fig.4.1 except for $U = 2$.

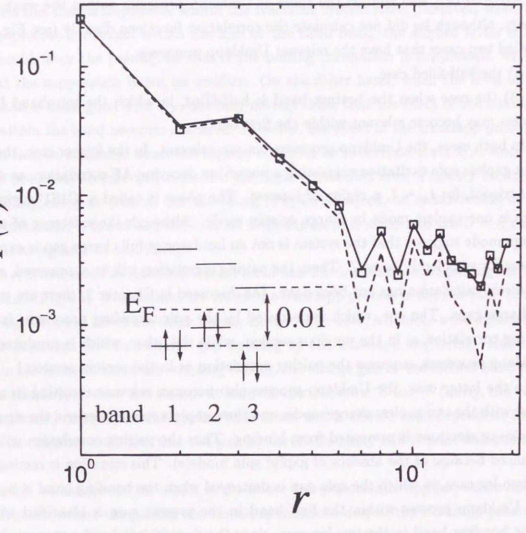

Figure 4.3: Similar plot as in Fig.4.1 for 38-rung system having 82 electrons for $U = 1$ with $t_{\perp} = 0.685$. The inset schematically depicts the positions of energy levels for the non-interacting case.

4.3 Effects of the Umklapp Processes

In this section, we discuss the effects of the Umklapp processes at special fillings to clarify the doping dependence. In the three-leg Hubbard model, the Umklapp processes can play an important role at specific band fillings.

Arrigoni[122] also studied the effect of Umklapp processes within the weak-coupling theory, although he did not calculate the correlation functions directly (see Fig.3.1). He studied two cases that have the relevant Umklapp processes.

(i) the half-filled case.

(ii) the case when the bottom band is half-filled, in which the intraband Umklapp process may become relevant within the first band.

In both cases, the Umklapp processes become relevant. In the former case, the system has a gapless spin excitation suggesting a power-law decaying AF correlation, as discussed by Arrigoni, for $t_\perp \sim t$, a region of interest. The phase is called a 'C1S1' regime, since there is one gapless mode in charge or spin mode. Although the existence of a gapless charge mode suggests that the system is not an insulator, a full charge gap is expected to appear for sufficiently large U. Then, the pairing correlation will be suppressed, although the direct calculation has not been done. (As discussed in Chapter 2, there are two kinds of charge gaps. The one, which is produced by the pair-tunneling processes, favors the pairing correlation as in the previous section, while the other, which is produced by the Umklapp processes, suppress the pairing correlation as in the present section.)

In the latter case, the Umklapp process also becomes relevant resulting in a 'C2S3' phase with the two gapless charge modes and three gapless spin modes and the singlet-pair of holes or electrons is prevented from binding. Thus the pairing correlation will be not enhanced because of the absence of gapful spin mode(s). This situation is reminiscent of the two-leg case, in which the spin gap is destroyed when the bonding band is half-filled. The Umklapp process within the first band in the present case is identified with that in the bonding band in the two-leg case, since the first (third) band corresponds to the bonding (anti-bonding) band as far as the pairing correlation is concerned as discussed in Chapter 3.

Given this situation, our motivation here is to look at the pairing correlation and, in addition, to explore in which case the Umklapp scattering does or does not affect the pairing correlation. We study the above two cases and also study the case in which the second band is half-filled. Namely, we wish to see whether both the first and the third bands, which involve the pairing order parameter, are affected by an indirect effect of the Umklapp process in the second band. Such a situation emerges in ladder systems with

three or larger number of legs.

We have tuned the value of $t_\perp$ to ensure that the level offset ($\Delta\varepsilon$) between the first and the third bands at the Fermi level is as small as O(0.01) for $U = 0$ to single out the effect of Umklapp processes from those due to large values of $\Delta\varepsilon$. Ideally, we should make the single electron energy levels of all the three bands lie close to each other around the Fermi level but that is impossible within the tractable system sizes. However, when the Umklapp process is relevant within the first or the third band, the aligned levels of the bands should favor the pairing, so that if the pairing correlation is suppressed, we can infer that the suppression is not an artifact. On the other hand, when the level of the second band is misaligned from E_F, one may naively think that the effect of the Umklapp process within the band becomes obscured. However, the effect of the Umklapp processes should in fact be enhanced when the highest occupied level derivate from E_F, since the Umklapp processes become well-defined if the highest occupied level is doubly occupied.

In the beginning we look at the half-filling (Fig.4.4). Indeed, no enhancement of the pairing correlation is found and the over all decaying form is similar to the $U = 0$ result as in the two-leg case at half-filling.

When n is decreased to make the second band half-filled, the enhanced pairing correlation is found (Fig.4.5). Possibilities are either the Umklapp process is not relevant, or it is relevant but does not affect the other bands. In the latter case, a density-wave correlation might be dominant due to a charge gap opening by the Umklapp scattering. However, at least in the sense of the weak-coupling theory, the charge gap in the second band only enhances the density-wave correlation at long distances from r^{-2} to r^{-1} (unity, the value of the exponent, comes from the gapless spin mode and it should be independent to U) in the weak-coupling limit and thus the pairing correlation may still remain dominant for small U.

Although we cannot decide which of the above two possibilities applies, we do have a unique situation where the pairing correlation is enhanced *despite* the Umklapp processes being possible. This interesting situation does not appear in the two-leg ladder.

Lastly, we study the case so that the first band is half-filled when n is further decreased and $t_\perp$ is also decreased (Fig.4.6). In this case, we again observe no enhancement in $P(r)$, as expected from the weak-coupling theory and the above discussion.

4.4 Summary

In this chapter, we have shown with the projector quantum Monte Carlo method that the enhancement of the pairing correlation expected from the results in the previous chapter

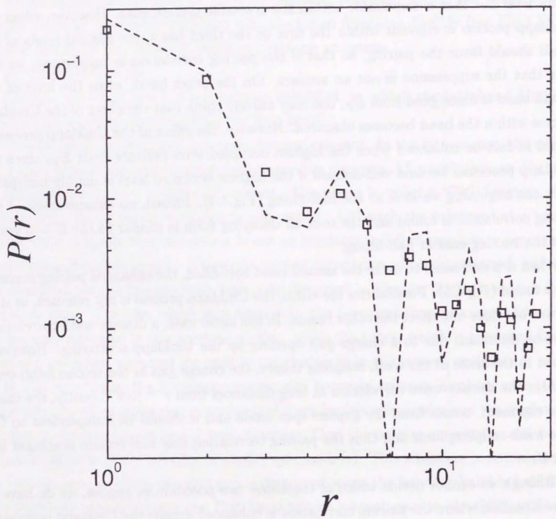

Figure 4.4: Pairing correlation $P(r)$ (□) against r for a 38-rung system for $U = 2$ with $t_\perp = 0.955$ and 114 electrons (half-filling). The dashed line represents the non-interacting result.

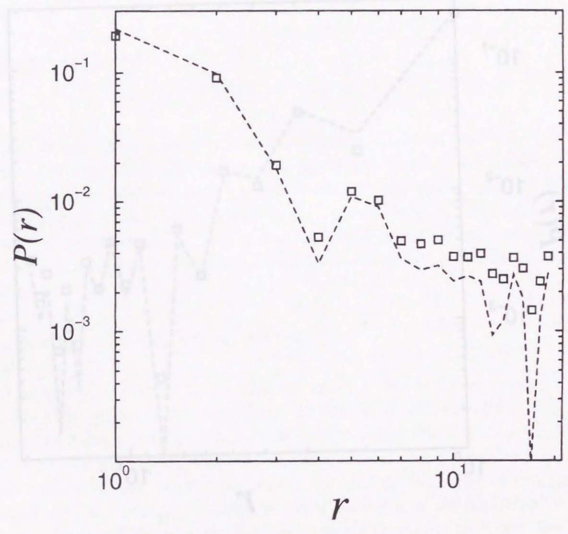

Figure 4.5: Pairing correlation $P(r)$ (□) against r for a 38-rung system for $U = 2$ with $t_\perp = 0.87$ and 110 electrons (the half-filled second band). The dashed line represents the non-interacting result.

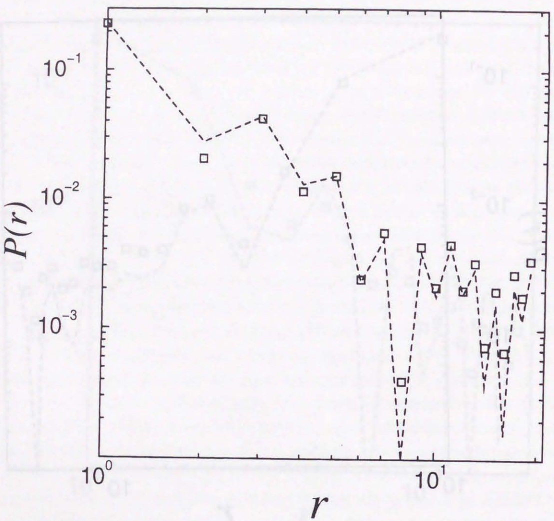

Figure 4.6: Pairing correlation $P(r)$ (□) against r for a 38-rung system for $U = 2$ with $t_\perp = 0.725$ and 74 electrons (the half-filled first band). The dashed line represents the non-interacting result.

is indeed found even for the intermediate interaction strengths($U \sim 2t$) and the interchain hoppings($t_\perp \sim t$). The features of the enhancement is similar to that in the two-leg case.

We have also studied the cases where the Umklapp processes can be relevant. Especially, we found that the enhancement of the pairing correlation is not affected by the intraband Umklapp process within the second band.

Chapter 5

Summary

In the present thesis, we have studied the pairing correlation in the Hubbard ladder model with an even(two) or an odd(three) number of legs. This has been motivated from a conjecture due to Rice et al. that an even-numbered ladder should exhibit dominance of the interchain singlet pairing correlation as expected from the persistent spin gap away from half-filling. Naively, one can then expect that an odd-numbered ladder should not exhibit dominance of the pairing correlation reflecting the presence of gapless spin excitations.

Two-leg ladder with a QMC method

We have considered the two-leg Hubbard ladder model. In the weak-coupling theory, in which the interactions are treated with the perturbative renormalization-group method, a d-wave like pairing correlation becomes dominant reflecting a spin gap in the two-leg Hubbard ladder. The relevant scattering processes are the pair-tunneling process across the bonding and the anti-bonding bands and the backward-scattering process within each band. The pair-tunneling process is reminiscent of the Suhl-Kondo mechanism for superconductivity in the transition metals with a two-band structure. However, the weak-coupling theory is correct only for infinitesimally small interactions in principle. Thus the calculation for finite interaction U is needed, but existing numerical calculations for finite U have been controversial.

In Chapter 2, we have applied the projector Monte Carlo method to look into the pairing correlation function in the ground state for finite U. We conclude that the discreteness of energy levels in finite systems affects the pairing correlation enormously, where the enhanced pairing correlation is indeed detected for intermediate interaction strengths if we tune the parameters so as to align the discrete energy levels of bonding and anti-bonding bands at the Fermi level in order to mimic the thermodynamic limit. The enhancement of the pairing correlation in the $U = 2t$ case is smaller than that in the $U = t$ case. This is consistent with the weak-coupling theory in which the pairing correlation decays as $r^{-1/(2K_\rho)}$ (K_ρ is the critical exponent of the gapless charge mode) at long distances and K_ρ is a *decreasing* function of U.

In the cases where interband or intraband Umklapp process is possible, the pairing correlation is not enhanced. This result is also consistent with the weak-coupling theory.

Three-leg ladder with the the weak-coupling theory

We then moved onto the correlation functions in the three-leg Hubbard ladder model in Chapter 3. Whether the above 'even-odd' conjecture holds for the simplest-odd ladder (i.e. the three-leg ladder) with a plural number of charge and spin modes is an important problem. This has remained an open question, since there had been no results for the pairing correlation function in the three-leg $t - J$ or Hubbard ladder models.

A key is the coexistence of gapless and gapful spin excitations in the doped three-leg Hubbard ladder. This has been analytically shown from the correlation functions starting from the phase diagram obtained by Arrigoni[122], who enumerated the numbers of the gapless charge and spin modes with the perturbative renormalization-group technique in the weak-coupling limit. If we turn to the correlation functions, we have found that the coexisting gapful and gapless modes give rise to a peculiar situation where a specific pairing *across* the central and edge chains (roughly a d-wave pairing) is dominant, while the $2k_F$ SDW on the edge chains simultaneously shows a subdominant but still long-tailed (power-law) decay associated with the gapless spin mode. The relevant scattering processes are the pair-tunneling process between the top and the bottom bands and the backward-scattering process within the top and the bottom bands. The situation is rather similar to the two leg case where the pair-tunneling processes play an important role for the enhanced pairing correlation. Schulz has independently obtained results for both the SDW and the pairing correlations which are similar to those given in Chapter 3 recently.

Three-leg ladder with a QMC method

However, as discussed in the two-leg case, it is not clear whether the weak-coupling results might be applicable only to infinitesimally small interaction strengths. In Chapter 4, we have thus checked the pairing correlation in the three-leg Hubbard ladder with

the QMC method tuning the parameters so as to align the discrete energy levels of the first and third bands at the Fermi level as in the two-leg case. The enhanced pairing correlation is indeed detected even for intermediate interaction strengths in the three-leg ladder. The enhancement of the pairing correlation in the $U = 2t$ case is smaller than that in the $U = t$ case as in the two-leg case in Chapter 2. This result is consistent with the weak-coupling theory in Chapter 3 in a similar reason with that in the two-leg case. Namely, the exponent of the pairing correlation is a decreasing function of K_ρ's which should decrease with U.

Various effects of the Umklapp processes have also been discussed.

Concluding remarks and future problems

The key message obtained in the present thesis, is that the dominance of the pairing correlation only requires the existence of gap(s) in not all but *some* of the spin modes. This is independent to whether the number of legs is even(two) or odd(three).

There are still important open questions. One is how the Hubbard model can possibly be related to real systems such as the cuprates. Specifically, One should study the two-leg and/or three-leg Hubbard ladder for larger U, where the dominance of the pairing correlation might be lost. Furthermore, the three-leg $t - J$ model should be studied to be compared with the Hubbard ladder. It would also be interesting to further look into ladder systems with larger numbers of legs.

Appendix A

Quantum Monte Carlo Method for the Ground State

After the work by Hirsh[130], who first applied the QMC method to the Hubbard model, some developments[30, 31, 32, 131] in the method enable us to study the ground state or the low temperature property of the Hubbard model[28, 29, 30, 31, 32] As we have seen in the present thesis, we can calculate the correlation functions in the system with relatively large numbers of sites by the QMC method. Here, we briefly describe the QMC method for ground states in the present thesis.

First we divide the Hamiltonian into the non-interacting and the on-site interaction parts,

$$\begin{aligned} H &= H_0 + H_{in}, \\ H_0 &= -t \sum_{i,\nu,\sigma} c^{\dagger}_{i,\nu,\sigma} c_{i+1,\nu,\sigma} - t_{\perp} \sum_{i,\nu,\sigma} c^{\dagger}_{i,\nu+1,\sigma} c_{i,\nu,\sigma}, \qquad \text{(A.1)} \\ H_{in} &= U \sum_{i,\nu} n_{i,\nu,\uparrow} n_{i,\nu,\downarrow}. \end{aligned}$$

The notations are standard and ν labels the legs. The ground state energy of the system can be generally written as

$$E_g = -\lim_{\beta\to\infty} \frac{1}{\beta} \log \frac{\rho(\beta+\delta\beta)}{\rho(\beta)}, \qquad \text{(A.2)}$$

$$\rho(\beta) = \langle \varphi_t | e^{-\beta H} | \varphi_t \rangle, \qquad \text{(A.3)}$$

where $|\varphi_t\rangle$ is the trial state, which must not be orthogonal to the ground state. By taking the limit $\beta \to \infty$, we can project out the ground state. In this sense the QMC method used in the present thesis is called the 'projector' quantum Monte Carlo method. To calculate $\rho(\beta)$, we decompose $\exp(-\beta H)$ by the Trotter formula as

$$\exp(-\beta H) = [\exp(-\Delta\tau H)]^L \quad (\Delta\tau = \beta/L), \qquad \text{(A.4)}$$

$$\exp(-\Delta\tau H) = \exp(-\Delta\tau H_0/2)\exp(-\Delta\tau H_{in})\exp(-\Delta\tau H_0/2) + O((\Delta\tau t)^3(U/t)), \quad (A.5)$$

where we assume $t_\perp \sim t$. Here, L should be taken sufficiently large so that $\Delta\tau$ is small. The error from the decomposition also increases with the interaction U. Thus we should take larger L for larger U. Next, we introduce the Stratonovich-Hubbard transformation of the Ising type to eliminate the non-bilinear term in each Trotter slice as

$$\exp[-\Delta\tau U n_{i,\nu,\uparrow} n_{i,\nu,\downarrow}] = \frac{1}{2}\sum_{s_{i\nu}=\pm 1} \exp[2as_{i\nu}(n_{i,\nu,\uparrow} - n_{i,\nu,\downarrow}) - \frac{U}{2}(n_{i,\nu,\uparrow} + n_{i,\nu,\downarrow})], \quad (A.6)$$

where a is defined as $\tanh(a) \equiv \sqrt{\tanh(U/4)}$. As a result, $\exp(-\Delta\tau H_{in})$ is rewritten as

$$\exp(-\Delta\tau H_{in}) = \sum_{\{s_{i\nu}\}} V(s_{11}, \cdots, s_{1N}, \cdots, s_{n1}, \cdots, s_{nN}). \quad (A.7)$$

Since $V(s)$ is written in terms of exp[linear combination of $\{n_{i,\nu,\sigma}\}$], we can rewrite $\rho(\beta)$ as

$$\rho(\beta) = \langle\varphi_t|e^{-\beta H}|\varphi_t\rangle = \sum_{\{s_{i\nu}(l)\}} \langle\varphi_t|X(\{s_{i\nu}(l)\};\beta)|\varphi_t\rangle, \quad (A.8)$$

where l denotes the Trotter slice. Here X is written as exp[linear combination of $\{n_{i,\nu,\sigma}\}$]. X and $|\varphi_t\rangle$ are represented by matrices using the single-particle basis and thus we can calculate $\langle\varphi_t|X(\{s_{i\nu}(l)\};\beta)|\varphi_t\rangle$ by taking the determinant of the corresponding matrix.

Next we consider the physical quantities such as the ground-state energy. In the beginning we define the probability function,

$$P(\{s_{i\nu}(l)\};\beta) = \frac{|W(\{s_{i\nu}(l)\};\beta)|}{\sum_{s_{i\nu}(l)} |W(\{s_{i\nu}(l)\};\beta)|}, \quad (A.9)$$

where W is defined as $W(\{s_{i\nu}(l)\};\beta) = \langle\varphi_t|X(\{s_{i\nu}(l)\};\beta)|\varphi_t\rangle$. The ground-state energy E_g in eq.(A.2) can be represented by the probability function as

$$\frac{\rho(\beta+\delta\beta)}{\rho(\beta)} = \frac{\sum_{\{s_{i\nu}(l)\}}\langle\varphi_t|X(\{s_{i\nu}(l)\};\beta+\delta\beta)|\varphi_t\rangle}{\sum_{\{s_{i\nu}(l)\}}\langle\varphi_t|X(\{s_{i\nu}(l)\};\beta)|\varphi_t\rangle} = \frac{\sum_{\{s_{i\nu}(l)\}} P(\{s_{i\nu}(l)\};\beta)\frac{W(\{s_{i\nu}(l)\};\beta+\delta\beta)}{|W(\{s_{i\nu}(l)\};\beta)|}}{\sum_{\{s_{i\nu}(l)\}} P(\{s_{i\nu}(l)\};\beta)\mathrm{sign}W(\{s_{i\nu}(l)\};\beta)}. \quad (A.10)$$

In order to generate the configurations of the Stratonovich variables, we flip the variable according to the probability,

$$p(s_{i\nu}(l) = 1 \rightarrow s_{i\nu}(l) = -1)$$

$$= \frac{P(\cdots, s_{i\nu}(l) = 1, \cdots; \beta)}{P(\cdots, s_{i\nu}(l) = 1, \cdots; \beta) + P(\cdots, s_{i\nu}(l) = -1, \cdots; \beta)}, = \frac{|W(\cdots, s_{i\nu}(l) = 1, \cdots; \beta)|}{|W(\cdots, s_{i\nu}(l) = 1, \cdots; \beta)| + |W(\cdots, s_{i\nu}(l) = -1, \cdots; \beta)|}, \quad (A.11)$$

which may be obtained without calculating $\sum_{s_{i\nu}(l)} |W(\{s_{i\nu}(l)\};\beta)|$ directly. Thus we can evaluate the ground-state energy using eq.(A.2). Other quantities such as the correlation functions can also be evaluated in the formalism.

Finally, we should give some comments on actual calculations. For large β which is necessary for the ground-state calculation, the number of matrix multiplications to obtain $\langle\varphi_t|X(\{s_{i\nu}(l)\};\beta)|\varphi_t\rangle$ becomes large and makes the calculation unstable. The orthogonalization procedure by Sorella et al.[30] may be used to circumvent the difficulty by orthonormalizing the resulting matrix once per several multiplications.

For large β, U, and system sizes, other difficulties also arise. One may easily see that the number of the Stratonovich variables increases linearly with that of the Trotter-slices L, which should increase with β, U, and the system sizes: we have taken $L \geq 5\beta U$ in the present study. Computation time required for one Monte Carlo step, which contains the update of all the Stratonovich variables, increases linearly with the number of the variables. Furthermore, for large numbers of Stratonovich variables, many Monte Carlo steps are needed for sufficient convergence of the simulation, resulting in a long computation time needed. Thus the tractable strength of U and the system sizes are restricted, since large β is necessary for the ground-state calculation.

On the other hand, the so-called *negative-sign problem* also arises for large β and/or U. Namely, the sample average of sign$W(\{s_{i\nu}\};\beta)$ tends to zero for large β and/or U. Since sign$W(\{s_{i\nu}\};\beta)$ is in the denominator in the right hand side of eq.(A.10), we have to evaluate $0/0$, which is numerically unstable. The difficulty also affects other physical quantities. We can relieve the difficulty by adopting the closed shell condition, in which there is no degeneracy in the single-particle state for non-interacting Fermi sea. Especially the negative-sign problem does not occur in the single chain case and/or at half-filling. However, the problem is often serious in multi-leg systems even in 1D because of the transfer between the chains.

Appendix B

Calculation Method in Chapter 3

B.1 Derivation of eq.(3.4)

Here we derive eq.(3.4) in the standard bosonization method. The intra- and the inter-band forward-scattering terms, which can be diagonally treated in the phase Hamiltonian as we will see in the following, are produced from the intrachain forward-scattering terms using eq.(3.3) as follows:

$$
\begin{aligned}
&\frac{2\pi v_F g}{L} \sum_{k_1,k_2,q} \sum_{\mu,\sigma,\sigma'} c^\dagger_{\mu,+,k_1,\sigma} c^\dagger_{\mu,-,k_2,\sigma'} c_{\mu,-,k_2+q,\sigma'} c_{\mu,-,k_1-q,\sigma} \\
&\quad \equiv H_{\mathrm{f}} + \text{pair-tunneling terms}, \\
&\quad = \frac{\pi v_F g}{4} \sum_{k_1,k_2,q} \sum_{\sigma,\sigma'} [3 a^\dagger_{1,+,k_1,\sigma} a^\dagger_{1,-,k_2,\sigma'} a_{1,-,k_2+q,\sigma'} a_{1,-,k_1-q,\sigma} \\
&\quad + 4 a^\dagger_{2,+,k_1,\sigma} a^\dagger_{2,-,k_2,\sigma'} a_{2,-,k_2+q,\sigma'} a_{2,-,k_1-q,\sigma} + 3 a^\dagger_{3,+,k_1,\sigma} a^\dagger_{3,-,k_2,\sigma'} a_{3,-,k_2+q,\sigma'} a_{3,-,k_1-q,\sigma} \\
&\quad + 2(a^\dagger_{1,+,k_1,\sigma} a^\dagger_{2,-,k_2,\sigma'} a_{2,-,k_2+q,\sigma'} a_{1,-,k_1-q,\sigma} + a^\dagger_{3,+,k_1,\sigma} a^\dagger_{2,-,k_2,\sigma'} a_{2,-,k_2+q,\sigma'} a_{3,-,k_1-q,\sigma} \\
&\quad + a^\dagger_{2,+,k_1,\sigma} a^\dagger_{1,-,k_2,\sigma'} a_{1,-,k_2+q,\sigma'} a_{2,-,k_1-q,\sigma} + a^\dagger_{2,+,k_1,\sigma} a^\dagger_{3,-,k_2,\sigma'} a_{3,-,k_2+q,\sigma'} a_{2,-,k_1-q,\sigma}) \\
&\quad + 3(a^\dagger_{1,+,k_1,\sigma} a^\dagger_{3,-,k_2,\sigma'} a_{3,-,k_2+q,\sigma'} a_{1,-,k_1-q,\sigma} + a^\dagger_{3,+,k_1,\sigma} a^\dagger_{1,-,k_2,\sigma'} a_{1,-,k_2+q,\sigma'} a_{3,-,k_1-q,\sigma})] \\
&\quad + \text{pair-tunneling terms}.
\end{aligned} \tag{B.1}
$$

Here H_{f} consists of the forward-scattering processes in the band description and the electron operator with index $+(-)$ belongs to the right-(left-) going branch. We prepare the following bosonic operators as in the usual single-chain case.

$$
\alpha_{i,k} = \begin{cases} \left(\frac{\pi}{kL}\right)^{1/2} \sum_{i,p,\sigma} a^\dagger_{i,+,p-k,\sigma} a_{i,+,p,\sigma} & \text{for } k > 0, \\ \left(\frac{\pi}{|k|L}\right)^{1/2} \sum_{i,p,\sigma} a^\dagger_{i,-,p+|k|,\sigma} a_{i,-,p,\sigma} & \text{for } k < 0, \end{cases} \tag{B.2}
$$

$$
\beta_{i,k} = \begin{cases} \left(\frac{\pi}{kL}\right)^{1/2} \sum_{i,p,\sigma} \sigma a^\dagger_{i,+,p-k,\sigma} a_{i,+,p,\sigma} & \text{for } k > 0, \\ \left(\frac{\pi}{|k|L}\right)^{1/2} \sum_{i,p,\sigma} \sigma a^\dagger_{i,-,p+|k|,\sigma} a_{i,-,p,\sigma} & \text{for } k < 0. \end{cases} \tag{B.3}
$$

$\alpha_{i,k}(\beta_{i,k})$ corresponds to the charge(spin)-density excitation in band i. Note that, $\alpha_{i,k}$ and $\beta_{i,k}$ obey the boson commutation relation:

$$[\alpha_{i,k}, \alpha_{i',k'}] = [\beta_{i,k}, \beta_{i',k'}] = [\alpha_{i,k}, \beta_{i',k'}] = [\alpha_{i,k}, \beta^{\dagger}_{i',k'}] = 0,$$

$$[\alpha_{i,k}, \alpha^{\dagger}_{i',k'}] = [\beta_{i,k}, \beta^{\dagger}_{i',k'}] = \delta_{i,i'}\delta_{k,k'}. \tag{B.4}$$

H_{f} is expressed in terms of only $\alpha_{i,k}$ as

$$\begin{aligned} H_{\mathrm{f}} &= \frac{v_F g}{4}\sum_{k>0} k[3(\alpha^{\dagger}_{1,k}\alpha^{\dagger}_{1,-k} + \alpha^{\dagger}_{3,k}\alpha^{\dagger}_{3,-k} + \alpha_{1,k}\alpha_{1,-k} + \alpha_{3,k}\alpha_{3,-k}) + 4(\alpha^{\dagger}_{2,k}\alpha^{\dagger}_{2,-k} + \alpha_{2,k}\alpha_{2,-k}) \\ &+ 2(\alpha^{\dagger}_{1,k}\alpha^{\dagger}_{2,-k} + \alpha_{1,k}\alpha_{2,-k} + \alpha^{\dagger}_{3,k}\alpha^{\dagger}_{2,-k} + \alpha_{3,k}\alpha_{2,-k} + \alpha^{\dagger}_{1,-k}\alpha^{\dagger}_{2,k} + \alpha_{1,-k}\alpha_{2,k} \\ &+ \alpha^{\dagger}_{3,-k}\alpha^{\dagger}_{2,k} + \alpha_{3,-k}\alpha_{2,k}) + 3(\alpha^{\dagger}_{1,k}\alpha^{\dagger}_{3,-k} + \alpha_{1,k}\alpha_{3,-k} + \alpha^{\dagger}_{3,k}\alpha^{\dagger}_{1,-k} + \alpha_{3,k}\alpha_{1,-k})]. \end{aligned} \tag{B.5}$$

Furthermore we can rewrite the non-interacting part of the Hamiltonian H_0 as

$$H_0 = v_F \sum_{i,p} |p|\alpha^{\dagger}_{i,p}\alpha_{i,p} + v_F \sum_{i,p} |p|\beta^{\dagger}_{i,p}\beta_{i,p}. \tag{B.6}$$

Now we introduce the phase variables as in the single chain case by the following equations:

$$\theta_{i\pm} = i\sum_{k>0}\sqrt{\frac{\pi}{Lk}}e^{-\Lambda k/2}[e^{-ikx}(\alpha^{\dagger}_{i,k} \pm \alpha_{i,-k}) - e^{ikx}(\alpha_{i,k} \pm \alpha^{\dagger}_{i,-k})], \tag{B.7}$$

$$\phi_{i\pm} = i\sum_{k>0}\sqrt{\frac{\pi}{Lk}}e^{-\Lambda k/2}[e^{-ikx}(\beta^{\dagger}_{i,k} \pm \beta_{i,-k}) - e^{ikx}(\beta_{i,k} \pm \beta^{\dagger}_{i,-k})]. \tag{B.8}$$

Here the phase variable $\phi_{i+}(\theta_{i+})$ can be regarded as the phase of the spin(charge)-density wave, while $\phi_{i-}(\theta_{i-})$ is the field dual to $\phi_{i+}(\theta_{i+})$.

From (B.7) and (B.8), we can write the diagonal part of the Hamiltonian, $H_{\mathrm{d}} = H_0 + H_{\mathrm{f}}$, in terms of the phase variables as

$$\begin{aligned} H_{\mathrm{d}} &= H_{\mathrm{spin}} + H_{\mathrm{charge}}, \\ H_{\mathrm{spin}} &= \sum_i \frac{v_F}{4\pi}\int dx[(\partial_x\phi_{i+})^2 + (\partial_x\phi_{i-})^2], \end{aligned} \tag{B.9}$$

$$\begin{aligned} H_{\mathrm{charge}} &= \frac{v_F}{4\pi}\int dx\Big[\big(1+\frac{3}{4}g\big)(\partial_x\theta_{1+})^2 + \big(1-\frac{3}{4}g\big)(\partial_x\theta_{1-})^2\Big] \\ &+ \frac{v_F}{4\pi}\int dx\Big[\big(1+g\big)(\partial_x\theta_{2+})^2 + \big(1-g\big)(\partial_x\theta_{2-})^2\Big] \\ &+ \frac{v_F}{4\pi}\int dx\Big[\big(1+\frac{3}{4}g\big)(\partial_x\theta_{3+})^2 + \big(1-\frac{3}{4}g\big)(\partial_x\theta_{3-})^2\Big] \end{aligned} \tag{B.10}$$

$$\begin{aligned} &+ \frac{v_F g}{4\pi}\int dx\Big[(\partial_x\theta_{1+})(\partial_x\theta_{2+}) - (\partial_x\theta_{1-})(\partial_x\theta_{2-}) + (\partial_x\theta_{3+})(\partial_x\theta_{2+}) - (\partial_x\theta_{3-})(\partial_x\theta_{2-})\Big] \\ &+ \frac{3v_F g}{8\pi}\int dx\Big[(\partial_x\theta_{1+})(\partial_x\theta_{3+}) - (\partial_x\theta_{1-})(\partial_x\theta_{3-})\Big]. \end{aligned} \tag{B.11}$$

Thus H_{d} is separated to both the spin-part H_{spin} and the charge-part H_{charge}. H_{charge} is also diagonalized by using eq.(3.5), while H_{spin} is already diagonalized. As a result, eq.(3.4) is easily obtained.

B.2 Calculation of Correlation Functions

Here we explain the method to derive the correlation functions. As examples, we here calculate the correlation functions of the intrachain singlet pairing in the edge chains and of the singlet pairing across the central and the edge chains. As stated in the text, the relevant scattering processes, are the pair-tunneling process between the first and the third bands and the backward-scattering process within the first or the third band.

The pair-tunneling process is expressed in terms of the phase variables as follows:

$$\begin{aligned} &\psi^{\dagger}_{3+\uparrow}\psi^{\dagger}_{3-\downarrow}\psi_{1-\downarrow}\psi_{1+\uparrow} + \psi^{\dagger}_{3+\downarrow}\psi^{\dagger}_{3-\uparrow}\psi_{1-\uparrow}\psi_{1+\downarrow} \\ +\ &\psi^{\dagger}_{3+\downarrow}\psi^{\dagger}_{3-\uparrow}\psi_{1+\uparrow}\psi_{1-\downarrow} + \psi^{\dagger}_{3+\uparrow}\psi^{\dagger}_{3-\downarrow}\psi_{1+\downarrow}\psi_{1-\uparrow} + \text{h.c.} \\ \propto\ &\eta_{3+\uparrow}\eta_{3-\downarrow}\eta_{1-\downarrow}\eta_{1+\uparrow}\exp[i(\theta_{1-} - \theta_{3-} + \phi_{1+} - \phi_{3+})] \\ +\ &\eta_{3+\downarrow}\eta_{3-\uparrow}\eta_{1-\uparrow}\eta_{1+\downarrow}\exp[i(\theta_{1-} - \theta_{3-} - \phi_{1+} + \phi_{3+})] \\ +\ &\eta_{3+\downarrow}\eta_{3-\uparrow}\eta_{1+\uparrow}\eta_{1-\downarrow}\exp[i(\theta_{1-} - \theta_{3-} + \phi_{1+} + \phi_{3+})] \\ +\ &\eta_{3+\uparrow}\eta_{3-\downarrow}\eta_{1+\downarrow}\eta_{1-\uparrow}\exp[i(\theta_{1-} - \theta_{3-} - \phi_{1+} - \phi_{3+})] + \text{h.c.}, \\ =\ &2\exp[i(\theta_{1-} - \theta_{3-})][\cos(\phi_{1+} - \phi_{3+}) - \cos(\phi_{1+} + \phi_{3+})] + \text{h.c.}, \\ =\ &8\cos(\sqrt{2}\chi_{1-})\sin(\phi_{1+})\sin(\phi_{3+}). \end{aligned} \tag{B.12}$$

Here we have defined the product of the U operators[55, 56] as $\eta_{i+\uparrow}\eta_{i-\downarrow} = \eta_{i+\downarrow}\eta_{i-\uparrow}$, but this convention does not affect the correlation functions as in the two-leg case[109, 111].

The backward-scattering process within band i is also expressed in terms of the phase variables through eq.(3.6) as

$$\begin{aligned} &\psi^{\dagger}_{i+\uparrow}\psi^{\dagger}_{i-\downarrow}\psi_{i+\downarrow}\psi_{i-\uparrow} + \text{h.c.} \\ =\ &\eta_{i+\uparrow}\eta_{i-\downarrow}\eta_{i+\downarrow}\eta_{i-\uparrow}\exp[-2i\phi_{i+}] + \text{h.c.}, \\ =\ &-2\cos(2\phi_{i+}). \end{aligned} \tag{B.13}$$

This and eq.(B.12) give the eq.(3.7) in the text. In the beginning we calculate the correlation function of the intrachain pairing in an edge chain (α chain). The order parameter is expressed in the band description as

$$O_{\mathrm{intraSS}} \equiv \psi_{\alpha+\uparrow}\psi_{\alpha-\downarrow} \sim \frac{1}{4}[\psi_{1+\uparrow}\psi_{1-\downarrow} + \psi_{3+\uparrow}\psi_{3-\downarrow} + 2\psi_{2+\uparrow}\psi_{2-\downarrow}], \tag{B.14}$$

where we have picked up only the two-particle operators whose correlations show power-law decay at long distances. The correlations of the other two-particle operators correlation decay exponentially due to the gapful field(s). We can rewrite the above equation in the phase variables as

$$
\begin{aligned}
& \psi_{1+\uparrow}\psi_{1-\downarrow} + 2\psi_{2+\uparrow}\psi_{2-\downarrow} + \psi_{3+\uparrow}\psi_{3-\downarrow} \\
\propto\ & \eta_{1+\uparrow}\eta_{1-\downarrow}\exp[i(\theta_{1-} + \phi_{1+})] + \eta_{3+\uparrow}\eta_{3-\downarrow}\exp[i(\theta_{3-} + \phi_{3+})] + 2\eta_{2+\uparrow}\eta_{2-\downarrow}\exp[i(\theta_{2-} + \phi_{2+})], \\
=\ & i\exp\Big\{i[(\frac{1}{\sqrt{2}}\chi_{1-} + \frac{1}{\sqrt{3}}\chi_{2-} + \frac{1}{\sqrt{6}}\chi_{3-}) + \phi_{1+}]\Big\} \\
& + i\exp\Big\{i[(-\frac{1}{\sqrt{2}}\chi_{1-} + \frac{1}{\sqrt{3}}\chi_{2-} + \frac{1}{\sqrt{6}}\chi_{3-}) + \phi_{3+}]\Big\} + 2i\exp[i(\theta_{2-} + \phi_{2+})], \\
=\ & i\exp\Big\{i[(\frac{\pi}{2} + \frac{1}{\sqrt{3}}\chi_{2-} + \frac{1}{\sqrt{6}}\chi_{3-}) + \frac{\pi}{2}]\Big\} \\
& + i\exp\Big\{i[(-\frac{\pi}{2} + \frac{1}{\sqrt{3}}\chi_{2-} + \frac{1}{\sqrt{6}}\chi_{3-}) + \frac{\pi}{2}]\Big\} + 2i\exp[i(\theta_{2-} - \phi_{2+})], \\
=\ & 2i\exp[i(\theta_{2-} - \phi_{2+})].
\end{aligned}
\tag{B.15}
$$

Here we have fixed $\phi_{1+} = \phi_{3+} = \pi/2$ and $\chi_{1-} = \pi/\sqrt{2}$ as discussed in the text and the terms containing the gapful fields are canceled out. Now we can calculate the correlation function:

$$
\begin{aligned}
& \langle O_{\mathrm{intraSS}}(x) O_{\mathrm{intraSS}}(0)\rangle \\
\propto\ & \langle \exp[i(\theta_{2-}(x) - \phi_{2+}(x))]\exp[i(\theta_{2-}(0) - \phi_{2+}(0))]\rangle, \\
=\ & \exp[-\frac{1}{2}\{\langle(\theta_{2-}(x) - \theta_{2-}(0))^2\rangle + \langle(\phi_{2+}(x) - \phi_{2+}(0))^2\rangle\}], \\
=\ & \exp[-\frac{2\pi}{3L}(\frac{1}{K^{*}_{\rho 2}} + \frac{2}{K^{*}_{\rho 3}} + 3)\sum_{k>0}\frac{e^{-\Lambda k}}{k}(1 - \cos kx)], \\
=\ & \exp[-\frac{1}{6}(\frac{1}{K^{*}_{\rho 2}} + \frac{2}{K^{*}_{\rho 3}} + 3)\log(1 + \frac{x^2}{\Lambda^2})], \\
\sim\ & x^{-\frac{1}{3}(\frac{1}{K^{*}_{\rho 2}} + \frac{2}{K^{*}_{\rho 3}}) - 1}.
\end{aligned}
\tag{B.16}
$$

Next we calculate the correlation function of the singlet pairing across the central and the edge chains. The order parameter is expressed as

$$
\begin{aligned}
O_{\mathrm{CESS}} &= (\psi_{\alpha+\uparrow} + \psi_{\gamma+\uparrow})\psi_{\beta-\downarrow} - (\psi_{\alpha+\downarrow} + \psi_{\gamma+\downarrow})\psi_{\beta-\uparrow}, \\
&\sim \psi_{1+\uparrow}\psi_{1-\downarrow} - \psi_{3+\uparrow}\psi_{3-\downarrow} - (\psi_{1+\downarrow}\psi_{1-\uparrow} - \psi_{3+\downarrow}\psi_{3-\uparrow}).
\end{aligned}
\tag{B.17}
$$

Here again we pick up only the two-particle operators whose correlations show power-law decay. In terms of the phase variables, the order parameter can be rewritten as

$$
\begin{aligned}
& \psi_{1+\uparrow}\psi_{1-\downarrow} - \psi_{3+\uparrow}\psi_{3-\downarrow} - \psi_{1+\downarrow}\psi_{1-\uparrow} + \psi_{3+\downarrow}\psi_{3-\uparrow} \\
\propto\ & \eta_{1+\uparrow}\eta_{1-\downarrow}\exp[i(\theta_{1-} + \phi_{1+})] - \eta_{3+\uparrow}\eta_{3-\downarrow}\exp[i(\theta_{3-} + \phi_{3+})] \\
& -\eta_{1+\downarrow}\eta_{1-\uparrow}\exp[i(\theta_{1-} - \phi_{1+})] + \eta_{3+\downarrow}\eta_{3-\uparrow}\exp[i(\theta_{3-} - \phi_{3+})], \\
=\ & i[\exp[i\{(\frac{1}{\sqrt{2}}\frac{\pi}{\sqrt{2}} + \frac{1}{\sqrt{3}}\chi_{2-} + \frac{1}{\sqrt{6}}\chi_{3-}) + \frac{\pi}{2}\}] \\
& -\exp[i\{(-\frac{1}{\sqrt{2}}\frac{\pi}{\sqrt{2}} + \frac{1}{\sqrt{3}}\chi_{2-} + \frac{1}{\sqrt{6}}\chi_{3-}) + \frac{\pi}{2}\}] \\
& -\exp[i\{(\frac{1}{\sqrt{2}}\frac{\pi}{\sqrt{2}} + \frac{1}{\sqrt{3}}\chi_{2-} - \frac{1}{\sqrt{6}}\chi_{3-}) - \frac{\pi}{2}\}] \\
& +\exp[i\{(-\frac{1}{\sqrt{2}}\frac{\pi}{\sqrt{2}} + \frac{1}{\sqrt{3}}\chi_{2-} + \frac{1}{\sqrt{6}}\chi_{3-}) - \frac{\pi}{2}\}], \\
=\ & -4i\exp[i(\frac{1}{\sqrt{3}}\chi_{2-} + \frac{1}{\sqrt{6}}\chi_{3-})].
\end{aligned}
\tag{B.18}
$$

Calculation of the interchain pairing correlation function is quite similar to that of the intrachain pairing correlation.

$$
\begin{aligned}
& \langle O_{\mathrm{CESS}}(x) O_{\mathrm{CESS}}(0)\rangle \\
\propto\ & \langle \exp[i(\frac{1}{\sqrt{3}}\chi_{2-}(x) + \frac{1}{\sqrt{6}}\chi_{3-}(x))]\exp[i(\frac{1}{\sqrt{3}}\chi_{2-}(0) + \frac{1}{\sqrt{6}}\chi_{3-}(0))]\rangle, \\
=\ & \exp[-\frac{1}{2}\{\frac{1}{3}\langle(\chi_{2-}(x) - \chi_{2-}(0))^2\rangle + \frac{1}{6}\langle(\chi_{3-}(x) - \chi_{3-}(0))^2\rangle\}], \\
\sim\ & x^{-\frac{1}{3}(\frac{1}{K^{*}_{\rho 2}} + \frac{1}{2K^{*}_{\rho 3}})}.
\end{aligned}
\tag{B.19}
$$

From above calculations, we can see that the interchain pairing exploits the charge gap and the spin gaps to reduce the exponent of the correlation function, in contrast to the intrachain pairing.

Bibliography

[1] H.K. Onnes, Leiden Comm.1206,1226 (1991).

[2] J. Bardeen, L.N. Cooper, and J.R. Schrieffer, Phys. Rev. **108**, 1175 (1957).

[3] Y. Takada, J. Phys. Soc. Jpn. **45**, 786 (1978); *ibid.* **51**, 63 (1982).

[4] K. Miyake, S. Schmitt-Rink, and C. M. Varma, Phys. Rev. B **34**, 6554 (1986).

[5] T. Moriya and Y. Takahashi, J. Phys. Soc. Jpn. **60**, 776 (1991); T. Moriya, Y. Takahashi, and K. Ueda, Physica C **185**, 114 (1991).

[6] J.G. Bednorz and K.A. Müller, Z. Phys. B **64**, 189 (1986).

[7] See, e.g., *Electronic Properties of high-T_c Superconductors, The Normal and the Superconducting State*, edited by W. Lang, H. Jodlbauer, P. Schaffarich, and H. Kuzmany (Springer-Verlag, Berlin/Vienna/New York).

[8] B. Batlogg, H. Takagi, H.L. Kao, and J. Kwo, in *Electronic Properties of high-T_c Superconductors, The Normal and the Superconducting State*, edited by W. Lang, H. Jodlbauer, P. Schaffarich, and H. Kuzmany (Springer-Verlag, Berlin/Vienna/New York).

[9] T. Ito, K. Takenaka, and S. Uchida, Phys. Rev. Lett. **70**, 3995 (1993).

[10] B. Bucher, P. Steiner, J. Karpinski, E. Kaldis, and P. Wachter, Phys. Rev. Lett. **70**, 2012 (1989).

[11] S. Uchida, T. Ido, H. Takagi, T. Arima, Y. Tokura, and S. Tajima, Phys. Rev. B **43**, 7942 (1991).

[12] J. Orenstein, G.A. Thomas, A. Millis, S.L. Cooper, D. Rapkine, T. Timusk, L. Schneemeyer, and J. Waszczak, Phys. Rev. B **42**, 6342 (1990).

[13] G.A. Thomas, J. Orenstein, D. Rapkine, M. Capizzi, A. Millis, R. Bhatt, L. Schneemeyer, and J. Waszczak, Phys. Rev. Lett. **61**, 1313 (1988).

[14] J.M. Harris, Y.F. Yan, and N.P. Ong, Phys. Rev. B **40**, 2239 (1989).

[15] S.E. Barrett, J.A. Martindale, D.J. Durand, C.H. Pennington, C.P. Slichter, T.A. Friedmann, J.P. Rice, and D.M. Ginsberg, Phys. Rev. Lett. **66**, 108 (1991).

[16] M. Takigawa, P.C. Hammel, R.H. Heffner, and Z. Fisk, Phys. Rev. B **39**, 7371 (1989).

[17] M. Matsumura, Y. Itoh, H. Yasuoka, and Y. Ueda, J. Phys. Soc. Jpn. **65**, 699 (1996).

[18] K. Yoshimura, T. Uemura, M. Kato, K. Kosuge, T. Imai, and H. Yasuoka, Hyperfine Interact. **79**, 867 (1993).

[19] See, e.g., E. Dagotto, Rev. of Mod. Phys **66**, 763 (1994); D.J. Scalapino, Phys. Rep. **250**, 329 (1995);

[20] P.W. Anderson, Science **235**, 1196 (1987).

[21] J. Hubbard, Proc. R. Soc. London, Ser A **243** 336 (1957).

[22] I.E. Dzyaloshinskii, Zh. Eksp. Teor. Fiz. **93**, 1487 (1987).

[23] H.J. Schulz, Europhys. Lett. **4** 609 (1987).

[24] I.E. Dzyaloshinskii and V.M. Yakovenko, Zh. Eksp. Teor. Fiz. **94**, 344 (1988).

[25] N.E. Bickers, D.J. Scalapino, and S.R. White, Phys. Rev. Lett. **62**, 961 (1989).

[26] N.E. Bickers and S.R. White, Phys. Rev. B **43**, 8044 (1991).

[27] G. Fano, F. Ortolani, and A. Parola, Phys. Rev. B **46**, 1048 (1992).

[28] M. Imada and Y. Hatsugai, J. Phys. Soc. Jpn. **58**, 3572 (1989).

[29] N. Furukawa and M. Imada, J. Phys. Soc. Jpn. **61**, 3331 (1992).

[30] S. Sorella, E. Tosatti, S. Baroni, R. Car, and M. Parrinello, Int. J. Mod. Phys. B **1**, 993 (1988).

[31] S.R. White, D.J. Scalapino, R.L. Sugar, E.Y. Loh, J.E. Gubernatis, and R.T. Scalettar, Phys. Rev. B **40**, 506 (1991).

[32] W. von der Linden, I. Morenstern, and H. de Raedt, Phys. Rev. B **41**, 4669 (1990).

[33] A. Moreo, Phys. Rev. B **45**, 5059 (1992).

[34] K. Kuroki, H. Aoki, T. Hotta, and Y. Takada, to be published in Phys. Rev. B.

[35] H. Fukuyama, Prog. of Theor. Phys. Supple. **108**, 287 (1992);

[36] Y. Suzumura, Y. Hasegawa, and H. Fukuyama, J. Phys. Soc. Jpn. **57**, 401, 2768 (1988);

[37] H. Fukuyama, Y. Hasegawa, and Y. Suzumura, Physica C **153-155**, 1630 (1988).

[38] E. Dagotto and J. Riera, Phys. Rev. Lett. **70**, 682 (1993).

[39] E. Dagotto, J. Riera, Y.C. Chen, A. Moreo, A. Nazarenko, F. Alcaraz, and F. Ortolani, Phys. Rev. B **49**, 3548 (1994).

[40] E. Dagotto, J. Riera, and A.P. Young, Phys. Rev. B **42**, 2347 (1990).

[41] E. Kaxiras and E. Manousakis, Phys. Rev. B **38**, 866 (1988).

[42] D. Poilblanc, J. Riera, and E. Dagotto, Phys. Rev. B **43**, 7899 (1991).

[43] D. Poilblanc, Phys. Rev. B **49**, 1477 (1994).

[44] H. Yokoyama and H. Shiba, J. Phys. Soc. Jpn. **57**, 2482 (1988).

[45] M. Imada, J. Phys. Soc. Jpn. **60**, 1877 (1991).

[46] M. Imada, Phys. Rev. B **48**, 550 (1993).

[47] M. Troyer, Phys. Rev. B **48**, 4002 (1993).

[48] S. V. Kivelson, V. Emery, and H.Q. Lin, Phys. Rev. B **42**, 6523 (1990).

[49] E. Dagotto and J. Riera, Phys. Rev. B **46**, 12084 (1992).

[50] See, e.g., J. Sólyom, Adv. Phys. **28**, 201 (1979).

[51] V.J. Emery, in *Highly Conducting One-Dimensional Solids*, ed. by J.T. Devreese *et al.* (Plenum, New York, 1979), p.247.

[52] H. Fukuyama and H. Takayama, in *Electronic Properties of Inorganic Quasi-One Dimensional Compounds*, ed. by P. Monçeau (D. Reidel, 1985), p.41.

[53] S. Tomonaga, Prog. Theor. Phys. **5**, 544 (1950).

[54] J. M. Luttinger, J. math. Phys. **4**, 1154 (1963).

[55] F.D.M. Haldane, J. Phys. C **14**, 2585 (1981).

[56] F.D.M. Haldane, Phys. Rev. Lett. **47**, 1840 (1981).

[57] H. Fram and V.E. Korepin, Phys. Rev. B **42**, 10553 (1990).

[58] N. Kawakami and S.K. Yang, Phys. Lett. A **148**, 359 (1990).

[59] E.H. Lieb and F.Y. Wu, Phys. Rev. Lett. **20**, 1445 (1990).

[60] B. Sutherland, Phys. Rev. B **12**, 3795 (1975).

[61] P. Schlottman, Phys. Rev. B **36**, 5177 (1987).

[62] P.A. Bares and G. Blatter, Phys. Rev. Lett. **64**, 2567 (1990).

[63] M. Ogata, M.U. Luchini, S. Sorella, and F. Assard, Phys. Rev. Lett. **66**, 2388 (1991).

[64] See, e.g., E. Dagotto and T.M. Rice, Science **271** 618 (1996) and references therein.

[65] H.J. Schulz, Phys. Rev. B **34**, 6372 (1986).

[66] F.D.M. Haldane, Phys. Lett. A **93**, 464 (1993).

[67] Y. Nishiyama, N. Hatano, and M. Suzuki, J. Phys. Soc. Jpn **64**, 1967 (1994).

[68] S.P. Strong and A.J. Millis, Phys. Rev. Lett. **69**, 2419 (1992).

[69] D.V. Kveshchenko, Phys. Rev. B **50**, 380 (1994).

[70] E. Dagotto, J. Riera, and D.J. Scalapino, Phys. Rev. B **45**, 5744 (1992).

[71] T. Barnes, E. Dagotto, J. Riera, and E.S. Swanson, Phys. Rev. B **47**, 3196 (1993).

[72] T. Barnes and J. Riera, Phys. Rev. B **50**, 6817 (1994).

[73] S.R. White, R.M. Noack, and D.J. Scalapino, Phys. Rev. Lett **73**, 886 (1994).

[74] M. Greven, R.J. Birgeneau, and U.-J. Wiese, Phys. Rev. Lett. **77**, 1865 (1996).

[75] S. Gopalan, T.M. Rice, and M. Sigrist, Phys. Rev. B **49**, 8901 (1994).

[76] D. Poilblanc, H. Tsunetsugu, and T.M. Rice, Phys. Rev. B **50**, 6511 (1994).

[77] N. Hatano and Y. Nishiyama, J. Phys. A **28**, 3911 (1995).

[78] M. Troyer, H. Tsunetsugu, and D. Würtz, Phys. Rev. B **50**, 13515 (1994).

[79] A.W. Sandvik, E. Dagotto, and D.J. Scalapino, Phys. Rev. B **53**, R2934 (1996).

[80] M. Azzouz, L. Chen, and S. Moukouri, Phys. Rev. B **50**, 6233 (1994).

[81] D.C. Johnston, J.W. Johnson, D.P. Goshom, and A.P. Jacobson, Phys. Rev. B **35**, 219 (1987).

[82] R.S. Eccleston, T. Barnes, J. Brody, and J.W. Johnson, Phys. Rev. Lett. **73**, 2626 (1994).

[83] Z. Hiroi, M. Azuma, M. Takano, and Y. Bando, J. Solid State Chem. **95**, 230 (1991).

[84] M. Azuma, Z. Hiroi, M. Takano, K. Ishida, Y. Kitaoka, Phys. Rev. Lett. **73**, 3463 (1994).

[85] K. Ishida, Y. Kitaoka, Y. Tokunaga, S. Matsumoto, K. Asayama, M. Azuma, Z. Hiroi, and M. Takano, Phys. Rev. B **53**, 2827 (1996).

[86] K. Ishida, Y. Kitaoka, K. Asayama, M. Azuma, Z. Hiroi, and M. Takano, J. Phys. Soc. Jpn. **63**, 3222 (1994).

[87] K. Kojima, A. Karen, G.M. Luke, B. Nachumi, W.D. Wu, Y.J. Uemura, M. Azuma, and M. Takano, Phys. Rev. Lett. **74**, 2812 (1995).

[88] Z. Hiroi and M. Takano, Nature **377**, 41 (1995).

[89] T.M. Rice, S. Gopalan, and M. Sigrist, Europhys. Lett. **23** 445 (1993); Physica B **199 & 200**, 378 (1992).

[90] H. Fukuyama, N. Nagaosa, M. Saito, and T. Tanimoto, J. Phys. Soc. Jpn. **65**, 2377 (1996).

[91] Y. Motome, N. Katoh, N. Furukawa, and M. Imada, J. Phys. Soc. Jpn. **65**, 1949 (1996).

[92] M. Sigrist, T.M. Rice, and F.C. Zhang, Phys. Rev. B **49**, 12058 (1994).

[93] D.V. Khveshchenko, Phys. Rev. B **50**, 380 (1994).

[94] D.V. Khveshchenko and T.M. Rice, Phys. Rev. B **50**, 252 (1994).

[95] H. Tsunetsugu, M. Troyer, and T.M. Rice, Phys. Rev. B **49**, 16078 (1994); *ibid* **51**, 16456 (1995).

[96] C.A. Hayward, D. Poilblanc, R.M. Noack, D.J. Scalapino, and W. Hanke, Phys. Rev. Lett. **75**, 926 (1995).

[97] C.A. Hayward and D. Poilblanc, Phys. Rev. B **53**, 11721 (1996).

[98] C.A. Hayward, D. Poilblanc, and D.J. Scalapino, Phys. Rev. B **53**, R8863 (1996).

[99] K. Sano, J. Phys. Soc. Jpn. **65**, 1146 (1996).

[100] Z. Hiroi and Y. Takano, Nature **377**, 41 (1995).

[101] M. Uehara, T. Nagata, J. Akimitsu, H. Takahashi, N. Môri, and K. Kinoshita, J. Phys. Soc. Jpn. **65**, 2764 (1996).

[102] N. Môri, H. Takahashi, and T. Nakanishi, Solid State Physics **31**, 797 (1996).

[103] A. Luther and V.J. Emery, Phys. Rev. Lett. **33**, 589 (1974).

[104] P.A. Lee, Phys. Rev. Lett. **34**, 1247 (1975).

[105] C.M. Varma and A. Zawadowski, Phys. Rev. B **32**, 7399 (1985).

[106] K. Penc and J. Sölyom, Phys. Rev. B **44**, 12690 (1993).

[107] A.M. Finkel'stein and A.I. Larkin, Phys. Rev. B **47**, 10461 (1993).

[108] L. Balents and M.P.A. Fisher, Phys. Rev. B **53**, 12133 (1996).

[109] M. Fabrizio, Phys. Rev. B **48**, 15838 (1993); M. Fabrizio, A. Parola, and E. Tosatti, Phys. Rev. B 46, 3159 (1992).

[110] N. Nagaosa and M. Oshikawa, J. Phys. Soc. Jpn. **65**, 2241 (1996).

[111] H.J. Schulz, Phys. Rev. B **53**, R2959 (1996).

[112] R.M. Noack, S.R. White, and D.J. Scalapino, Phys. Rev. Lett. **73**, 882 (1994).

[113] R.M. Noack, S.R. White, and D.J. Scalapino, preprint (cond-mat/9601047).

[114] H. Suhl, B.T. Mattis, and L.R. Walker, Phys. Rev. Lett. **3**, 552 (1959).

[115] J. Kondo, Prog. Theor. Phys. **29**, 1 (1963).

[116] K.A. Muttalib and V.J. Emery, Phys. Rev. Lett. **57**, 1370 (1986).

[117] K. Yamaji and Y. Shimoi, Physica C **222**, 349 (1994); K. Yamaji, Y. Shimoi, and T. Yanagisawa, Physica C **235-240**, 2221 (1994).

[118] Y. Asai, Phys. Rev. B **52**, 10390 (1995).

[119] S.R. White and D.J. Scalapino, preprint (cond-mat/9605143).

[120] K. Kuroki, T. Kimura, and H. Aoki, Phys. Rev. B, R15641 (1996).

[121] T. Kimura, K. Kuroki, and H. Aoki, Phys. Rev. B **54**, R9608 (1996).

[122] E. Arrigoni, Phys. Lett. A **215**, 91 (1996).

[123] H.J. Schulz, preprint (cond-mat/965075).

[124] T. Kimura, K. Kuroki, and H. Aoki, submitted to Phys. Rev. B, preprint (cond-mat/9610200).

[125] R.M. Noack, S.R. White, and D.J. Scalapino, Europhys. Lett. **30**, 163 (1995); J. Low Temp. Phys. **99**, 593 (1995).

[126] M.S. Hybertsen, E.B. Stechel, M. Schlüter, and D.R. Jennison, Phys. Rev. B **41**, 11068.

[127] S. Bacci, E. Gagliano, R. Martin, and J. Annett, Phys. Rev. B **44**, 7504 (1991).

[128] N.M. Bogoliubov and V.E. Korepin, Int. J. Mod. Phys. **3**, 427 (1989).

[129] L.D. Landau, Soviet Phys. JETP **3**, 920 (1957); Soviet Phys. **5**, 101 (1957); Soviet Phys. **8**, 70 (1958).

[130] J.E. Hirsh, Phys. Rev. B **31**, 4403 (1985).

[131] G. Sugiyama and S.E. Konin, Ann. Phys. **168**, 1 (1986).

偶奇本梯子系における超伝導の理論的研究